

EXPERIMENTAL DISSERTATION

PAILIN FANCY COLOUR SAPPHIRES a.k.a TALILA

献给我的父亲

TABLE OF CONTENTS

Introduction

1. Corundum and the Pailin gemfield

1.1 Colours in corundum

1.2 Pailin and its corundum

1.2.1 Pailin blue sapphires

1.2.2 Talila sapphires

1.2.3 Pailin geology and mines

2. Sampling

3. Experimental methods

3.1 Basic instruments

3.2 Spectroscopy

3.2.1 UV – Vis – NIR

3.2.2 Fourier Transform Infrared Spectroscopy (FTIR)

3.2.3 Parallel faces

3.3 Chemical analysis

4. Results

4.1 Basic gemmology

4.1.1 Test summary

4.1.2 Microscope observation

4.2 Spectroscopy

4.2.1 UV – Vis – NIR

4.2.2 FTIR

4.3 Chemistry

5. Discussion

5.1 Colours of the sapphires

5.1.1 Purple category

5.1.2 Pink category

5.1.3 Blue category

5.1.4 Colour-zoning in sample SW2

5.2 Geological origin of these sapphires

5.2.1 Metamorphic or basaltic?

5.2.2 Questions raised

5.3 3,309 cm⁻¹ peak and its interpretation

Conclusion

Acknowledgements

References

Annex

INTRODUCTION

Searching for gemstones in Pailin, Cambodia, I was offered a few years ago to buy “talila” sapphires (figure 1). I had never heard of that name before and was curious about it. The lot was composed of hundreds of round stones whose colours were mainly pink to purple with many different hues. Some were darker or greyer than others, and the whole lot gave an interesting range of colours. Blue sapphires were not introduced in these lots, and colourless, green and yellow sapphires are seldom seen in Pailin. The stones were faceted (brilliant or mixed cut), and the rough crystals were rounded. Going on a regular basis to Pailin, I buy “talila” sapphires on every trip. Overtime I have grown increasingly curious about these gemstones and got the urge to know much more about them as I could not find the word “talila” in any literature. Indeed, the term appears to be very local and I have not heard it outside of Pailin and Chanthaburi area. In all other places, they are referred to as fancy colour sapphires. I asked myself different questions about them:

- Where do their colour come from? Local dealers often emphasize they contain chromium. How far is this true?
- Why is it specific to this area? Can they be found in other places?
- What is their geological origin?



Figure 1: “talila” sapphires

1. CORUNDUM AND THE PAILIN GEMFIELDS

1.1 COLOURS IN CORUNDUM

Corundum, in its pure state, is composed of 40% aluminum and 60% oxygen, its chemical composition is Al_2O_3 . Aluminum is a trivalent cation (Al^{3+}) and oxygen a divalent anion (O^{2-}). When it is a perfect crystal, with absolutely no impurity or defect, corundum does not absorb any light and is thus colourless. Indeed, its band gap is about 9.5 eV (Emmett et al., 2017). However, one site of Al^{3+} out of three is not occupied in the lattice, thus some impurities can take an Al^{3+} vacant site. These impurities may include:

- trivalent chromium (Cr^{3+}), it is a chromophore, i.e. it is a cause of colour in corundum. Indeed, Cr^{3+} is known to give rise to red and pink colour (Fritsch et al. 1987),
- trivalent iron, or ferric iron (Fe^{3+}) is another chromophore that gives rise to a yellow colour – isolated and / or in pair (Fritsch et al. 1987),
- divalent iron (ferrous iron, Fe^{2+}) and tetravalent titanium (Ti^{4+}) are involved in a charge transfer ($\text{Fe}^{2+} - \text{O}^{2-} - \text{Ti}^{4+}$) that gives a blue colour. Another charge transfer gives a blue colour and involves ferrous and ferric iron: $\text{Fe}^{2+} - \text{O}^{2-} - \text{Fe}^{3+}$ (Fritsch et al., 1988).

1.2 PAILIN AND ITS CORUNDUM

Pailin is located in the far west of Cambodia, about 20 kilometres from the Thai border (figure 2). The city remained quite secluded as up to 2010, no paved road was linking it to Battambang when 4 hours were needed to complete this 80 kilometre-journey.



Figure 2: Pailin province on a Cambodian Map

1.2.1 PAILIN BLUE SAPPHIRES

Pailin has been well known for its blue sapphires. Even, if they are not as famous as Kashmir, Ceylon and Burma sapphires, Pailin blue sapphires are well known. They extend from light blue to dark blue. They show a distinctive rich blue colour, referred to as “royal blue”. However, they do not look inky as do many basalt, iron-rich sapphires (figure 3).



Figure 3: a 2.68ct Pailin blue sapphire. Left picture taken without flash, right picture taken with a flash

Pailin sapphires are characterized by crystals surrounded by secondary healed fractures, plagioclase feldspar, and certainly the most characteristic solid inclusion is uranium pyrochlore having a reddish-orange octahedron look (Figure 4).



Figure 4: a tiny red octahedral of uranium pyrochlore in a Cambodian sapphire. Photographer: E. Billie Hughes. Taken on internet from Lotus gemology hyperion database (www.lotusgemology.com/index.php/library/inclusion-gallery?filter%5Bgemtype%5D=Natural+Sapphire&filter%5Borigin%5D=Cambodia&filter%5Benhancement%5D=&filter%5Bsearch%5D=&start=0&layout=gallery#lg=1&slide=2). Also in Hughes, 2017

It is quite common for sapphires to be heated in Pailin (normal heat), more advanced treatment, such as beryllium-diffusion, are carried out in Chanthaburi (Thailand). Some rubies are also found in Pailin but much more rarely than sapphires. Nowadays, even blue sapphires are hard to find in Pailin, and when available they hardly exceed two carats (ct) in size. One has to be very cautious as a lot of materials offered in Pailin actually come from Africa and Madagascar.

1.2.2 “TALILA” SAPPHIRES

The “talila” sapphires (figure 9) are found in the river and the alluvial deposits near Phnom O Tang (figure 5), and Phnom Ko Ngoap in older times (see below). Blue sapphires, are rarely seen in these areas. Indeed, they are found more in the Eastern part of Pailin. However, from time to time, some rubies are found at these locations. The crystals retrieved are rounded and range in colour from pink to purple (lilac, lavender, mauve...). According to a local dealer, the name “talila” comes from Thai language meaning sunset. The “talila” is found in small size, most of the material is faceted as round brilliant or mixed cut. The size ranges approximately between 3 to 5 mm, and the weight between 0.1 to 0.5 ct.

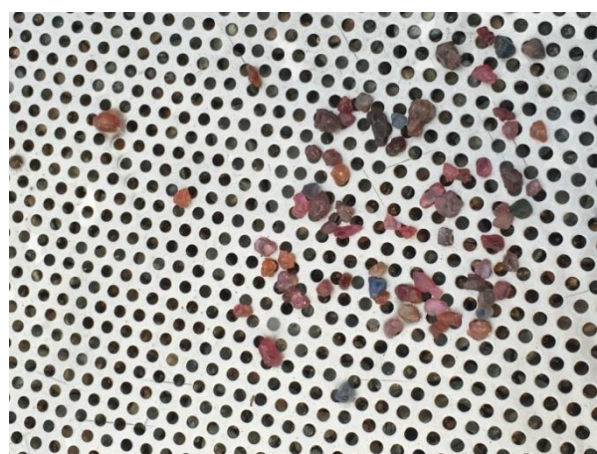


Figure 5: river mining (left), rough crystals found in the river (right)

Local dealers, emphasizes on their chromium-content.

One year ago, it was quite easy to find “talila” sapphires. Since January, they have become rarer and the individual size in the lots offered decreased. I regularly send few samples to a laboratory in Bangkok which, so far, has always confirmed the absence of treatment and the Cambodian origin of the “talila”.

1.2.3 PAILIN GEOLOGY AND MINES

Most of this section has been written with the help of two articles by Berrangé and Jobbins (Berrangé et al., 1976; Berrangé et al., 1981). Geologically speaking, Pailin is located along a fault zone having a northwest – southeast direction (Berrangé et al., 1976). This fault separates Pailin into two areas:

- one northern area with a low relief having ancient Precambrian crystal complex as well as Devonian and Carboniferous rocks,
- one southern mountainous areas composed of Triassic sandstones and greywackes, known as the Tadeth mountains. During the formation of Himalaya, Tadeth mountains were uplifted and small gem bearing basaltic bodies were intruded close to the fault zone with some extrusion of lavas. Eventually, weathering and erosion created the current alluvial deposits in rivers (Berrangé et al., 1976).

In the same study, Berrangé and Jobbins identified basalt rocks as the primary source of gemstones (Figure 6). Thanks to fission-track dating of zircons derived from the Pailin lavas, these rocks are estimated to age between 2.60 and 1.73 million years. Thus, they belong to rocks formed during the Cenozoic era.



Figure 6: Pailin basalt rocks

The Cenozoic basalt rocks contain inclusions of corundum along with zircon, spinel, garnet, ilmenite, magnetite, phlogopite and other minerals. All these inclusions are considered as xenocryst.

The lavas formed four separated hills (figure 7):

- Phnom O Tang lavas: a crater rising 40-60 metres above the plains, located 5-6 kilometres northwest of Pailin,
- Phnom Ko Ngoap lavas: a plateau (1x3 kilometres) rising 20-40 metres above the plains located 4-5 kilometres west of the city,
- Phnom Yat lavas: a plateau (600 metres x 3 kilometres) on which Pailin lies. At its southern part is Phnom Yat itself (254 metres), where no mining is carried out due to

- its being considered a holy place. However, I have noticed that a lot of people were looking there for gemstones after a storm, even though they did not dig,
- the fourth lava has been reported in a coffee plantation between Phnom Yat and Phnom Ko Ngoap. However, mining has not been reported there for decades. (Berrangé et al., 1981).

Alluvial deposits are generally near the original vent (about a 1 kilometre radius), for the river, the placers can be further away.



Figure 7: mining activity in Pailin province

Note that no mining activity has been reported for years at Phnom Ko Ngoap. Another area, Phnom Trop, about 20 kilometers south of Pailin in Tadeth mountains, has been mined with mitigating success (Pardieu, 2009). The last time I went there, it seems that mining at Phnom Trop was discontinued.

During my last trip to Pailin, no official mines were in activity. Indeed, the only official mines, Russian-Cambodian and Korean-Cambodian joint ventures, stopped their operation recently. Only illegal mines are in operation (figure 8), and such activity is tolerated only for Cambodian mine owners. Others, including Thai, had faced tough financial consequences when they tried to operate.



Figure 8: an illegal mine in Bo Tansu area. Blue sapphires are mainly found in this alluvial deposit

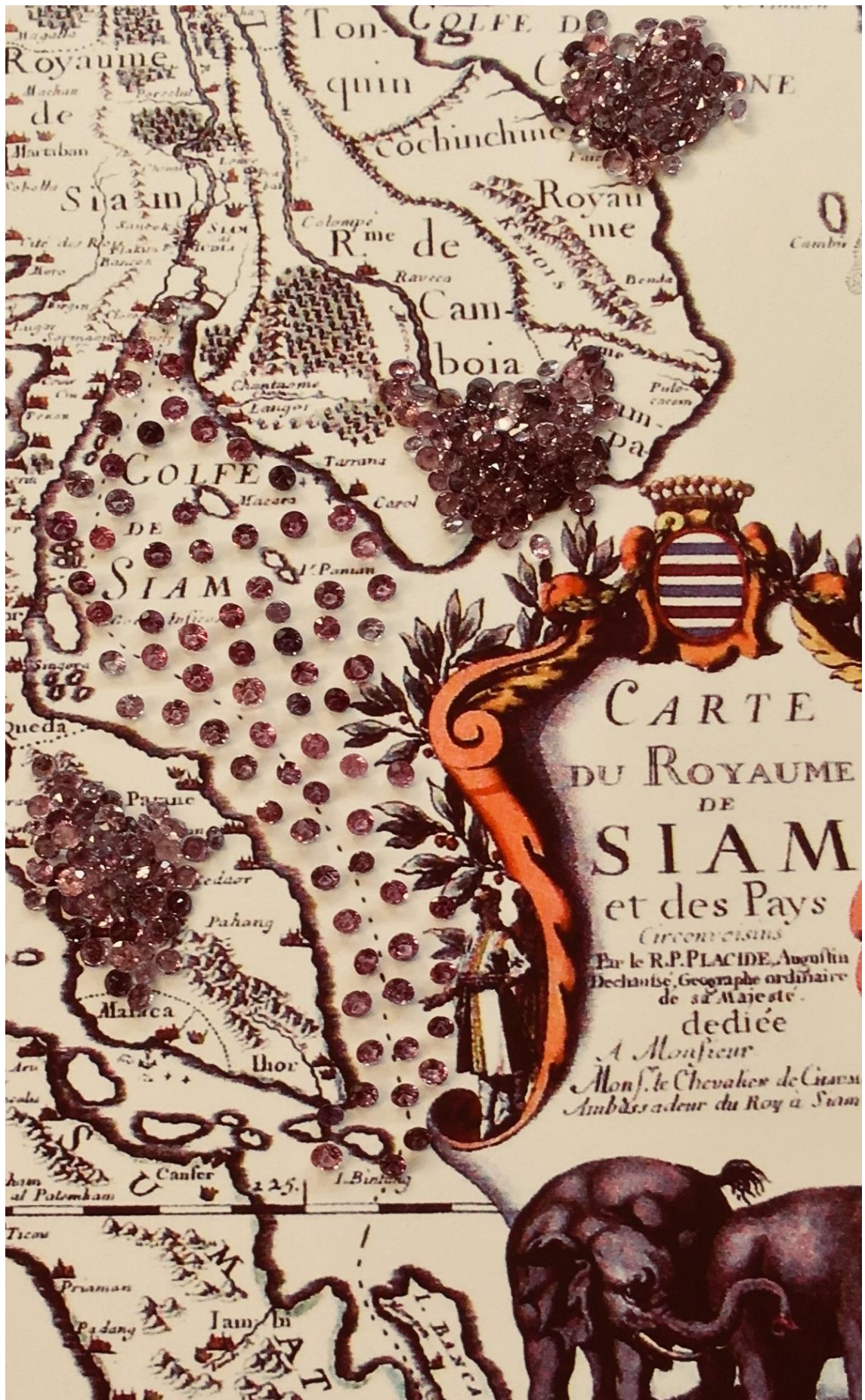


Figure 9: "talila" sapphires. Map of Siam and its circumvolving neighbor by R.P Augustin Placide. ©BNF

2. SAMPLING

Sapphires (figure 15) were selected to display the full range of colours seen in “talila” from pink to purple (figure 10). Some materials are darker (figure 11) or greyer (figure 12) than others. The stones are faceted, round brilliant and mixed cut. They are quite small, approximately 3 to 4.3 mm in diameter. One particularity encountered in Pailin is the absence of colourless, yellow and green materials, which are very rare. Table 1 gives a quick description of the sapphires.



Figure 10: classical colours seen in talila sapphires
Samples #SW8, SW10, SW11, SW12, SW13, SW14, SW15, SW16, SW18

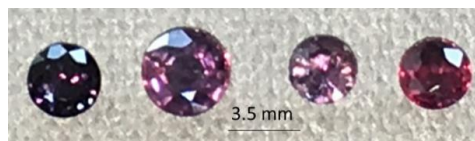


Figure 11: some darker colours seen in “talila” sapphires
Samples #SW1, SW2, SW6, SW9

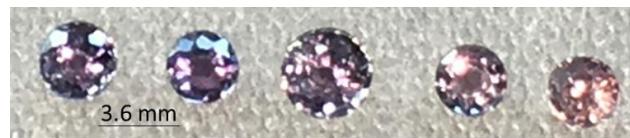


Figure 12: some greyer colours seen in “talila” sapphires
Samples #SW3, SW4, SW5, SW7, SW17

I also add two blue sapphires to be compared (figure 13). One of the two blue sapphires (SW19) is rarely encountered in Pailin, as it shows a strong yellowish brown / blue colour zoning. Its appearance looks typical of basaltic sapphires of the BGY series (blue, green, yellow). The other one is blue.

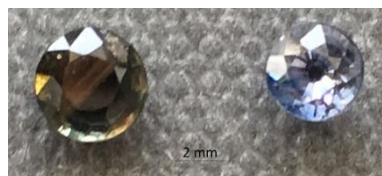


Figure 13: blue sapphires from Pailin
Samples #SW19 and SW20

Note, that sample SW2 (figure 14) which has a purple colour actually displays an interesting colour zoning of pink and blue.



Figure 14: sample SW2 seen face up (left) displaying a purple colour, the same sample seen from bottom side showing colour zoning (pink / blue)

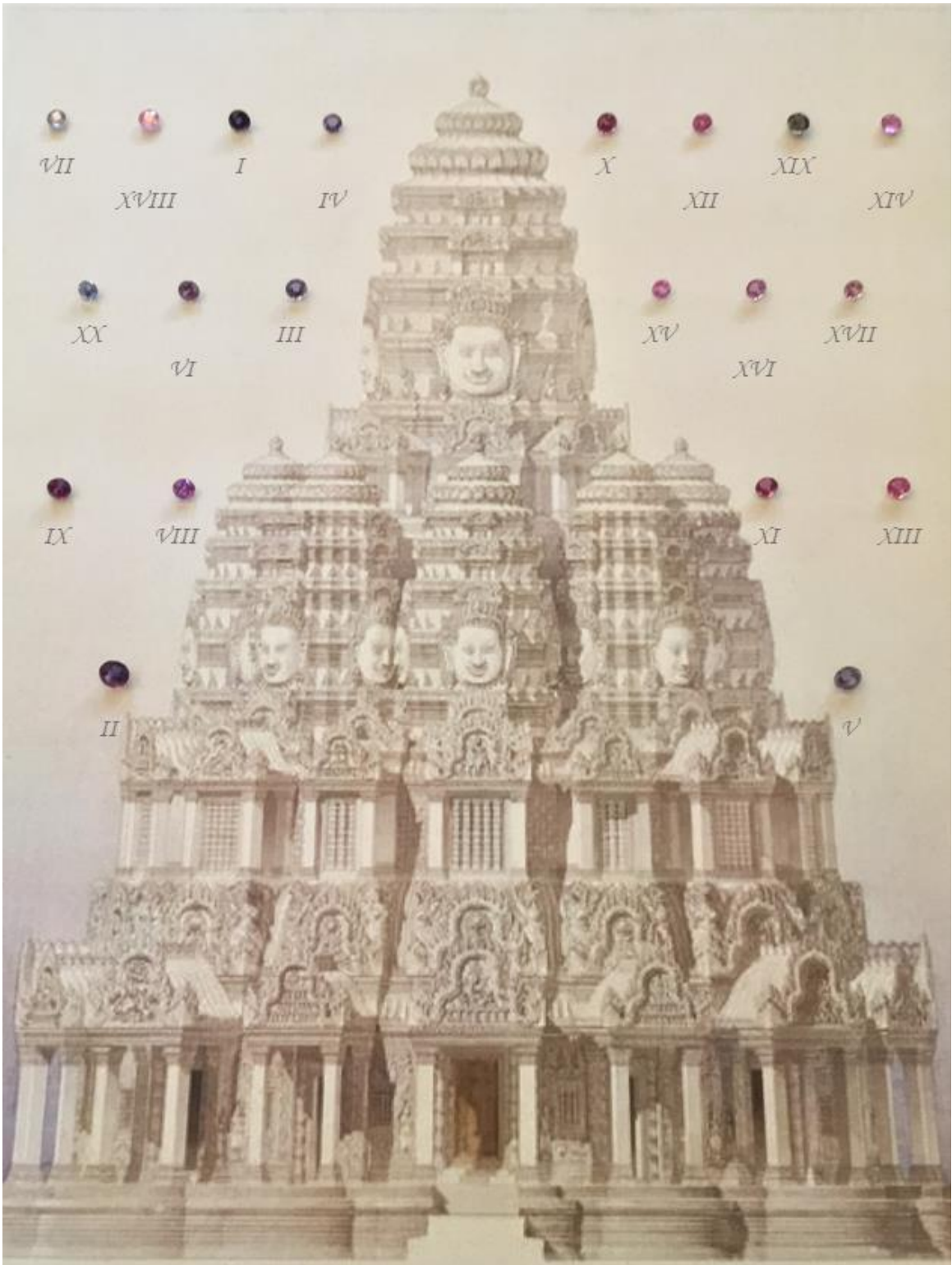


Figure 15: "talila" sapphires used in this study. Drawing by Joseph-Henri Deverin, falsely attributed to Louis Delaporte. Artistic reproduction of Bayon central tower. ©RMN

Sample	Picture	Colour	Avg. diameter (mm)	Depth (mm)	Weight (ct)	Comments
SW1		dark bluish purple	3.55	1.99	0.222	
SW2		purple	4.29	2.32	0.399	pink / blue colour zoning
SW3		bluish purple	3.32	2.00	0.207	
SW4		light purple	3.09	1.48	0.138	
SW5		light purplish grey	3.90	2.33	0.318	
SW6		purple	3.32	1.99	0.189	
SW7		light purplish grey	3.05	1.43	0.141	
SW8		pinkish purple	3.31	2.01	0.193	
SW9		dark pinkish purple	3.52	2.34	0.252	
SW10		purplish pink	3.36	2.33	0.234	
SW11		light brownish pink	3.31	2.02	0.228	
SW12		brownish pink	3.15	2.00	0.154	
SW13		brownish pink	3.30	1.99	0.199	
SW14		purplish pink	3.21	1.48	0.154	
SW15		pink	3.00	1.58	0.114	
SW16		light pinkish purple	3.21	1.98	0.181	
SW17		light greyish pink	3.02	1.91	0.127	
SW18		light yellowish pink	3.34	1.54	0.157	
SW19		brownish blue	3.57	1.89	0.244	yellowish brown / blue colour zoning
SW20		blue	3.06	2.32	0.168	

Table 1: description of the samples used in this study

The material obtained for this study was bought in Pailin in September 2016 from a trusted seller. I was assured that the material is not heated and comes from Pailin. As a regular customer, I have never taken this seller cheating, and until now he has always disclosed the treatments when they were present, and has always been honest with the geographic origin

of the stones. From time to time, I have sent stones he had sold me to a laboratory in Bangkok, and the results always come back in line with his words.

3. EXPERIMENTAL METHODS

To perform tests on the sapphires different equipment were used from the simplest to more sophisticated machines.

3.1 Basic instruments

First of all, the basic instruments of gemmology were used. They include, the use of microscope, of hand-held diffraction grating spectroscope, refractometer, polariscope and conoscope, London dichroscope, Chelsea colour filter, and ultra-violet cabinet (long wave ultra-violet – LWUV – at 365 nm, and short wave ultra-violet – SWUV – at 254 nm; the gems were placed on a dark background at approximately 7 centimeters (cm) from the bulbs).

3.2 Spectroscopy

Spectroscopy for this study used UV-Vis-NIR (ultraviolet – visible – near infrared) and Fourier transform infrared (FTIR) spectrometres.

3.2.1 UV-Vis-NIR

UV-Vis-NIR spectroscopy has been used to determine the origin of colour in the sapphires. The spectra were recorded in absorbance on a Perkin Elmer Lambda 1050. Spectral resolution is 1 nm. Photomultiplier tubes (PMT) detector is set with a slit of 1 nm (response 0.20 s and an auto gain) from 300 to 860 nm. Indium-gallium-arsenide (InGaAs) detector is set with a slit of 2 nm (response 0.40 s and a 5 gain) from 860 to 1,500 nm. Spectra were later manually set (Excel) in absorption coefficient to allow comparison between samples.

3.2.2 FTIR

FTIR spectroscopy has been used to determine the OH, and / or aluminum oxyhydroxide inclusions. Background and spectra were performed at room temperature using Bruker Vertex 70. Spectra were recorded in absorbance mode in the range 7,000 to 400 cm^{-1} . The spectral resolution chosen was 4 cm^{-1} . Spectra were later manually set (Excel) in absorption coefficient to allow comparison between samples. Most of spectra were done using 100 scans; some spectra having too much noise were redone with 1,000 scans without success.

3.2.3 PARALELL FACES

For both UV-Vis-NIR and FTIR spectroscopy appeared the problem of testing faceted gemstones. Indeed, as the samples are very small, it was quite impossible to find two parallel faces for the light path. As a result, the spectra were heavily noisy and unusable. To overcome this problem, the culet has been truncated to create a face which is parallel to the table. Despite this, a few spectra recorded on the FTIR spectrometer were too noisy to be used.

3.3 Chemical analysis

To study the colour and the origin of a gemstone, it is quite important to make a chemical analysis of minor and trace elements. This was performed using the energy dispersive spectroscopy (EDS) of the scanning electron microscope (SEM). The SEM used is a JEOL JSM-5800.

Two issues were encountered using the SEM. Firstly, some electronic charges of the samples prevented any analysis to be done (figure 16). I understood that this issue has been overcome since by a thorough cleaning of the metallizing equipment (Rondeau B., 2017, personal communication).

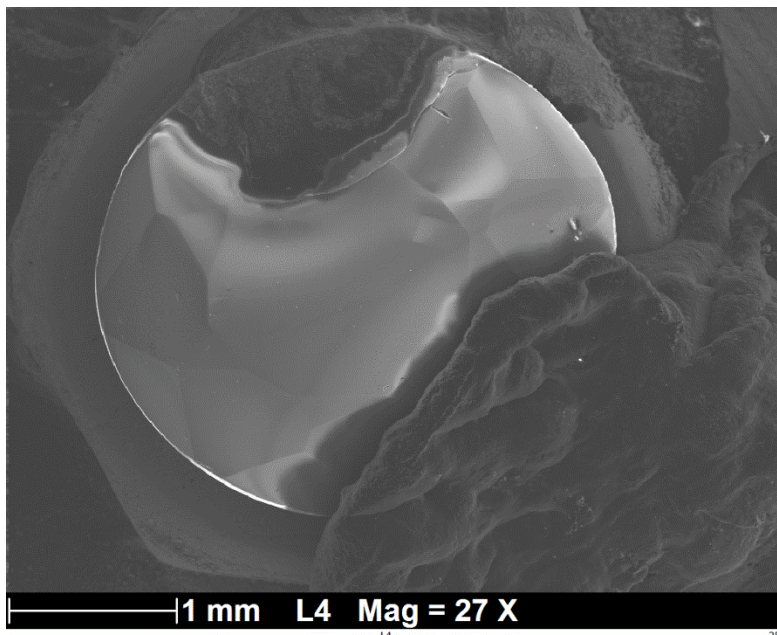


Figure 16: electronic charge on sample SW4 under SEM (secondary electrons)

The second issue is linked to the equipment itself. Indeed, the EDS function of SEM is not a suitable technique for the analysis of minor and trace elements (Fritsch E., 2017, personal communication).

To avoid these issues, the samples were sent to the Laboratoire Français de Gemmologie (LFG) in Paris to be analyzed by energy-dispersive X-ray fluorescence (EDXRF). I deeply wish to thank Ms. Annabelle Herreweghe who performed the analysis for me, as I could not go to Paris and do it myself. The analysis was performed on a Rigaku NEXCG CG1035. The unit used is oxide weight percent (% mass). Experiments were performed using energy levels from 25 kV to 50 kV, depending on the elements (the heavier, the higher the energy level).

4. RESULTS

4.1 Basic gemmology

4.1.1 TEST SUMMARY

Before using any advanced instruments, basic gemmological tests were conducted. The main results are summarized in table 2. The reading of the refractive index (RI) on the polariscope revealed that all the gemstones are uniaxial negative. Results of polariscope tests are not summarized in this table as the results were the same for all the materials, going light and dark four times through a complete rotation (360°). Moreover, tests with the conoscope revealed that for the 20 stones the uniaxial pattern.

The results of these basic gemmology tests are consistent with corundum optical properties.

Sample	Picture	Ω -ray	ϵ -ray	DR	Pleochroism	Chelsea filter	LWUV	SWUV
SW1		1.770	1.762	0.008	strong purple/yellow	pinkish red	inert	inert
SW2		1.770	1.761	0.009	strong blue / greenish yellow (on blue) and pink / yellowish orange (on pink)	pinkish red	weak red	inert
SW3		1.770	1.762	0.008	strong purple / greenish yellow	none	inert	inert
SW4		1.770	1.762	0.008	medium purple / yellowish	pinkish red	very weak red	inert
SW5		1.769	1.761	0.008	strong purple / greenish yellow	none	inert	inert
SW6		1.768	1.760	0.008	weak purple / yellowish purple	none	weak red	inert
SW7		1.769	1.761	0.008	strong purple / greenish yellow	none	very weak red	inert
SW8		1.770	1.762	0.008	strong purple / pale yellow	pinkish red	strong red	medium chalky blue
SW9		1.769	1.761	0.008	medium purple / yellowish orange	dark red	very weak red	inert
SW10		1.773	1.763	0.010	medium purple / yellowish orange	pinkish red	very weak red	very weak red
SW11		1.772	1.762	0.010	medium purplish pink / yellowish orange	dark red	very weak red	inert
SW12		1.772	1.762	0.010	medium purplish pink / yellowish orange	pinkish red	weak to medium red	inert
SW13		1.772	1.763	0.009	medium purplish pink / orangy yellow	pinkish red	weak red	inert
SW14		1.771	1.762	0.009	weak pinkish / orangy yellow	red	weak red	inert
SW15		1.771	1.761	0.010	medium to weak pink / pinkish yellow	pinkish red	strong red	medium chalky blue
SW16		1.772	1.763	0.009	medium light purplish pink / yellow	pinkish red	weak red	very weak red
SW17		1.769	1.761	0.008	medium light purplish pink / pale yellow	none	very weak red	inert
SW18		1.770	1.762	0.008	medium to weak light pink / pale yellow	pinkish red	medium red	inert
SW19		1.768	1.760	0.008	strong to medium blue / green	none	inert	inert
SW20		1.770	1.762	0.008	weak pale blue / pale greyish green	slightly green	very weak purple	inert

Table 2: Ω -ray: refractive index of the ordinary ray, ϵ -ray: refractive index of the extraordinary ray, DR: birefringence, LWUV: reaction to long wave ultraviolet (365nm), SWUV: reaction to short wave ultraviolet (254nm)

4.1.2 MICROSCOPE OBSERVATION

Observation through a microscope revealed that the inclusions are the ones found in natural corundum. Therefore, no synthetic material was detected (a doubt was possible when a strong red fluorescence is seen under LWUV for samples SW8 and SW15). The inclusions such as needles (figure 18), solid inclusions (crystals, figure 17), partially healed fractures (figure 17) were not modified giving evidence of an absence of heat treatment.

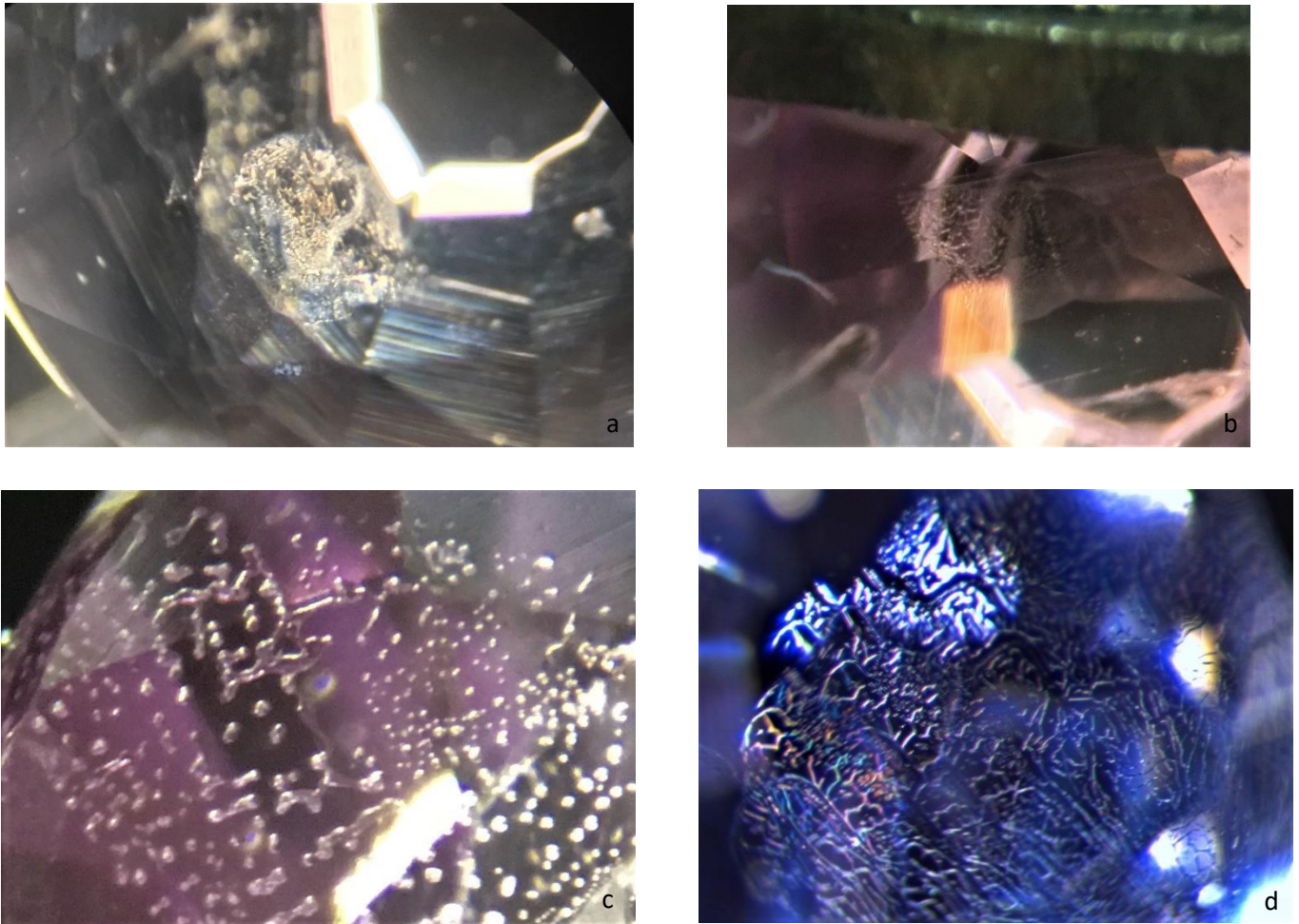
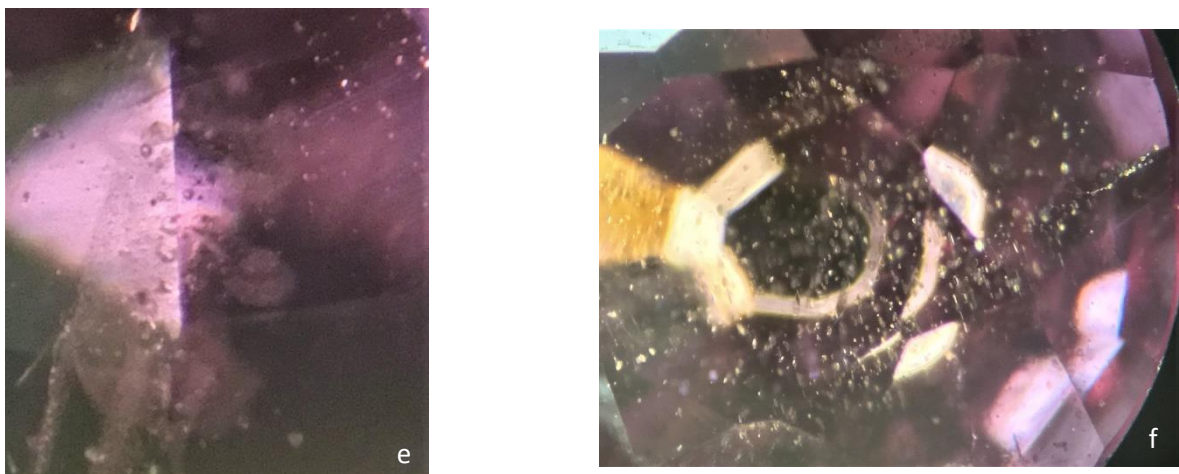


Figure 17: top: unaltered partially healed in fractures in samples SW5 (a) – SW13 (b) – SW15 (c) – SW20 (d). Darkfield and 60x magnification (a, b, c), darkfield and diffuse overhead fiber optic – 40x magnification (d).

Bottom: unmodified crystal inclusions in samples SW9 (e) and SW12 (f). Darkfield – 60x magnification



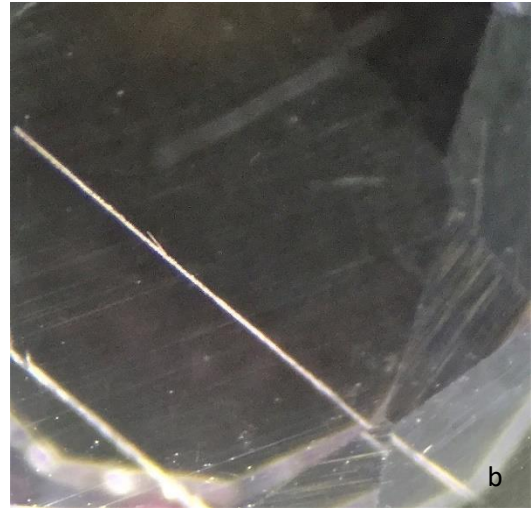
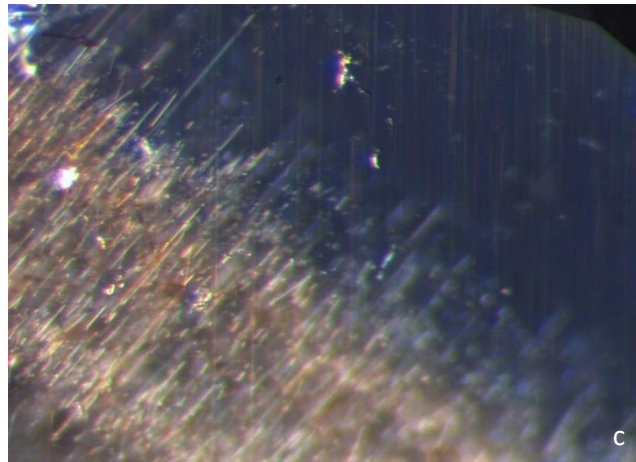


Figure 18: top: long coarse parallel needles in samples SW7 (a) and SW7 (b). Darkfield – 60x magnification. Bottom: oriented needles in sample SW19 (c). Darkfield and diffuse overhead fiber optic – 40x magnification



Twinning has also been detected (figure 19).

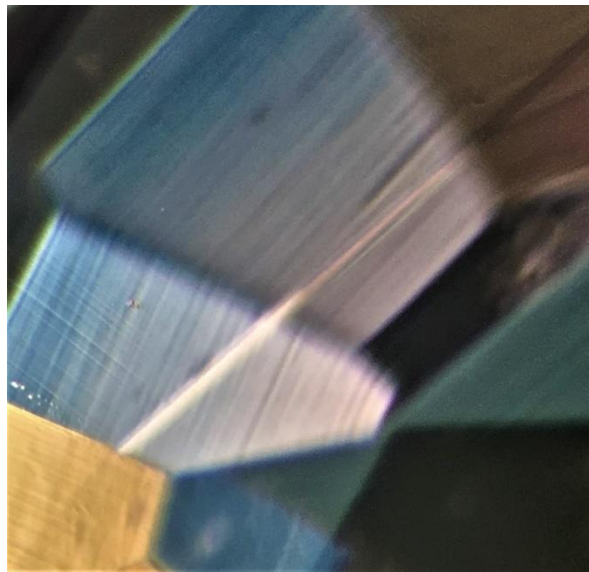


Figure 19: twinning in sample SW10. Darkfield and crossed polarizers – 60x magnification

4.2 Spectroscopy

4.2.1 UV-Vis-NIR

Trivalent iron is present in most of the spectra as single ions or pairs (Fe^{3+} , and $\text{Fe}^{3+}\text{-Fe}^{3+}$), such as trivalent chromium (Cr^{3+}) which is found in all spectra except the blue (SW20 might show a little bit of chromium, but is hardly visible in absorption coefficient). The presence of inter-valence charge transfer (IVTC) $\text{Fe}^{2+}\text{-O}^{2-}\text{-Ti}^{4+}$ is, in some cases, more difficult to assess. 12 samples also display a shoulder at about 330 nm which reflects a relatively high iron-content (Sutherland et al., 1998).

Four different types of spectrum can be identified:

- 1st type (figure 20): Fe^{3+} is present in single ion and in pairs (peak at about 388 nm for single Fe^{3+} ions, and peaks at ~ 377 and 450 nm for $\text{Fe}^{3+}\text{-Fe}^{3+}$ pairs). Cr^{3+} is present with a peak at about 694 nm and a large band approximately centred at 560 nm. This band at 560 nm is stacked with inter-valence charge transfer (IVCT) $\text{Fe}^{2+}\text{-O}^{2-}\text{-Ti}^{4+}$,

When too many spectra are stacked on the same figure (figure 20-b and 20-c), a representative spectrum has been isolated (figure 20-a).

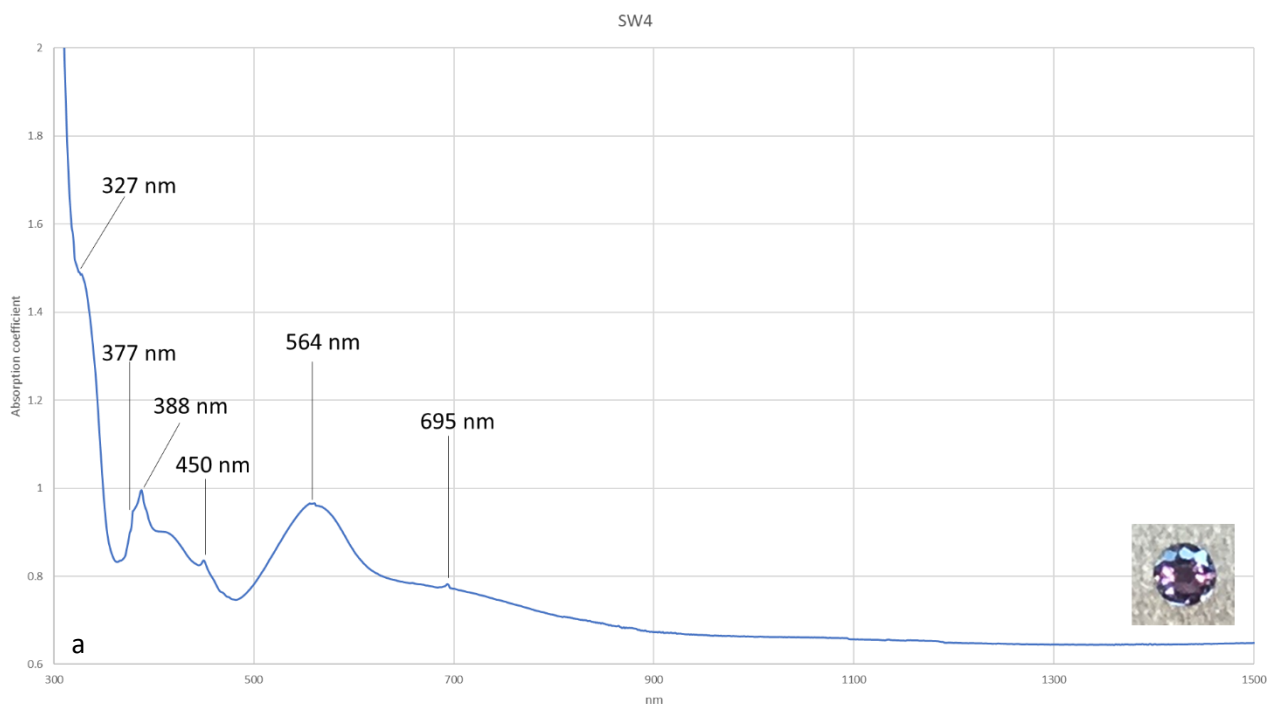


Figure 20-a: sample SW4 showing a spectrum with Fe^{3+} present as $\text{Fe}^{3+}\text{-Fe}^{3+}$ pairs (377 and 450 nm) and single Fe^{3+} ion (388nm), Cr^{3+} at 695 nm and stacked in the large band at 564 nm with $\text{Fe}^{2+}\text{-O}^{2-}\text{-Ti}^{4+}$

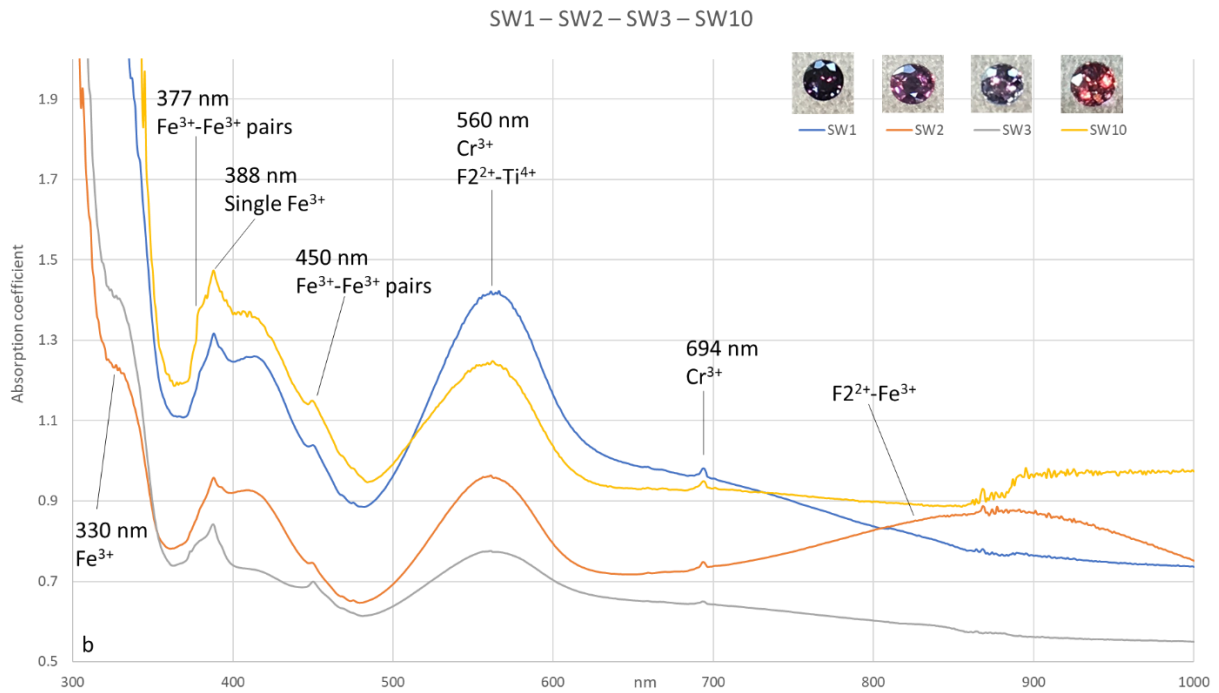


Figure 20-b: samples SW1 – SW2 – SW3 – SW10 showing the same features as SW4 (a). Note the broad band of $\text{Fe}^{2+}\text{-O}^{2-}\text{-Fe}^{3+}$ in SW2, it is the only one to show this charge transfer (except for SW20 which is blue)

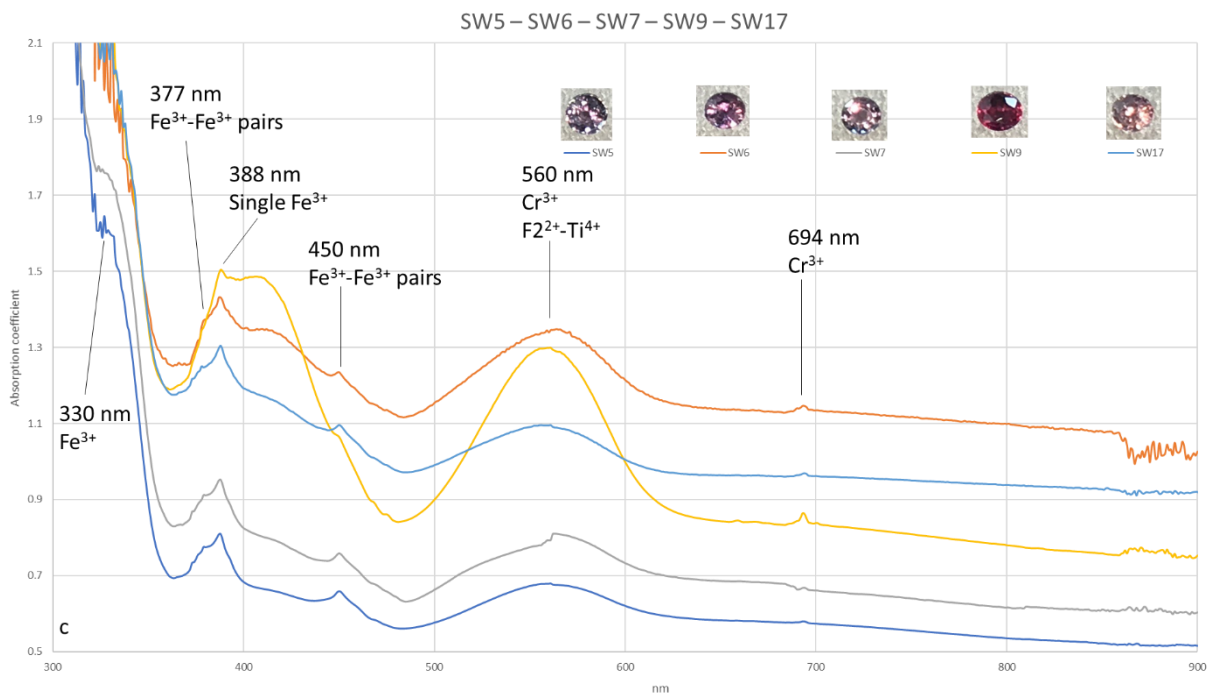


Figure 20-c: samples SW5 – SW6 – SW7 – SW9 – SW17 showing the same features as SW4 (a)

- Second type (figure 21): Fe^{3+} is present in single ion and in pairs (peak at about 388 nm for single Fe^{3+} ions, and peaks at ~ 377 and 450 nm for $\text{Fe}^{3+}\text{-Fe}^{3+}$ pairs). Cr^{3+} is present with a peak at about 694 nm and a large band approximately centred at 560 nm. The presence of $\text{Fe}^{2+}\text{-O}^{2-}\text{-Ti}^{4+}$, if any, is much lesser than in the first category

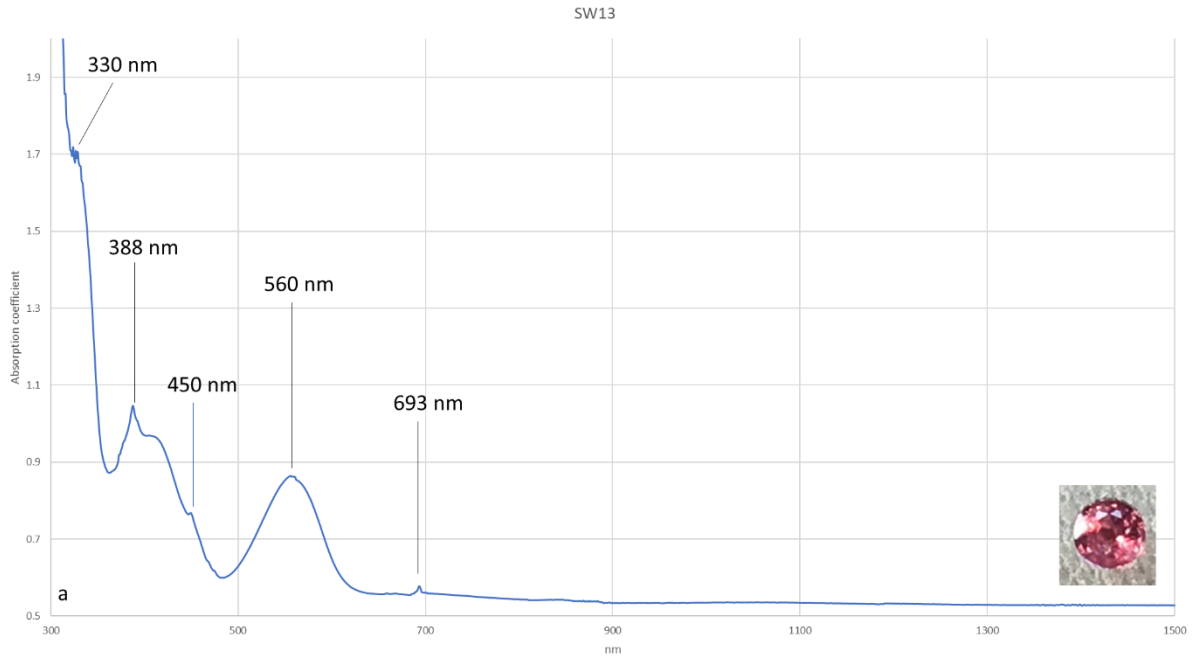


Figure 21-a: sample SW13 showing a spectrum with Fe^{3+} present as $\text{Fe}^{3+}\text{-Fe}^{3+}$ pairs (377 and 450 nm) and single Fe^{3+} ion (388nm), Cr^{3+} at 695 nm and in the large band at 560 nm with much less, if any, $\text{Fe}^{2+}\text{-O}^{2-}\text{-Ti}^{4+}$ as in the 1st type

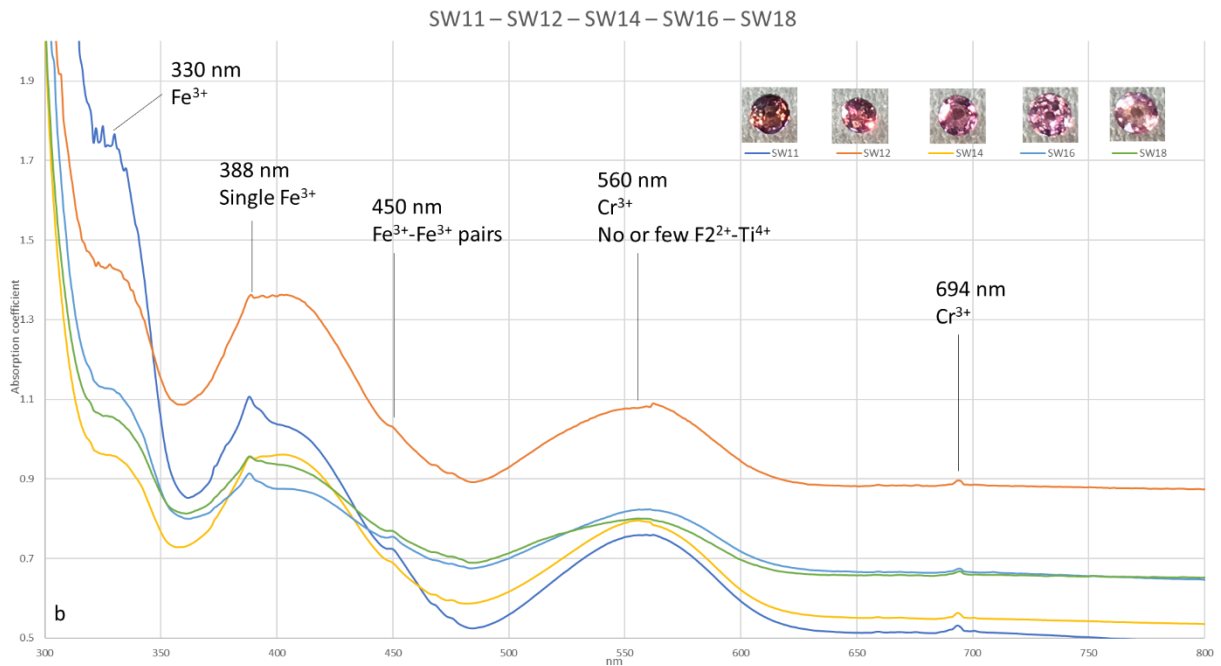


Figure 21-b: samples SW11 – SW12 – SW14 – SW16 – SW18 showing the same features as SW13 (a)

- 3rd type (figure 22): Cr³⁺ is highly dominant even though in one sample it is stacked with Fe²⁺-O²⁻-Ti⁴⁺,

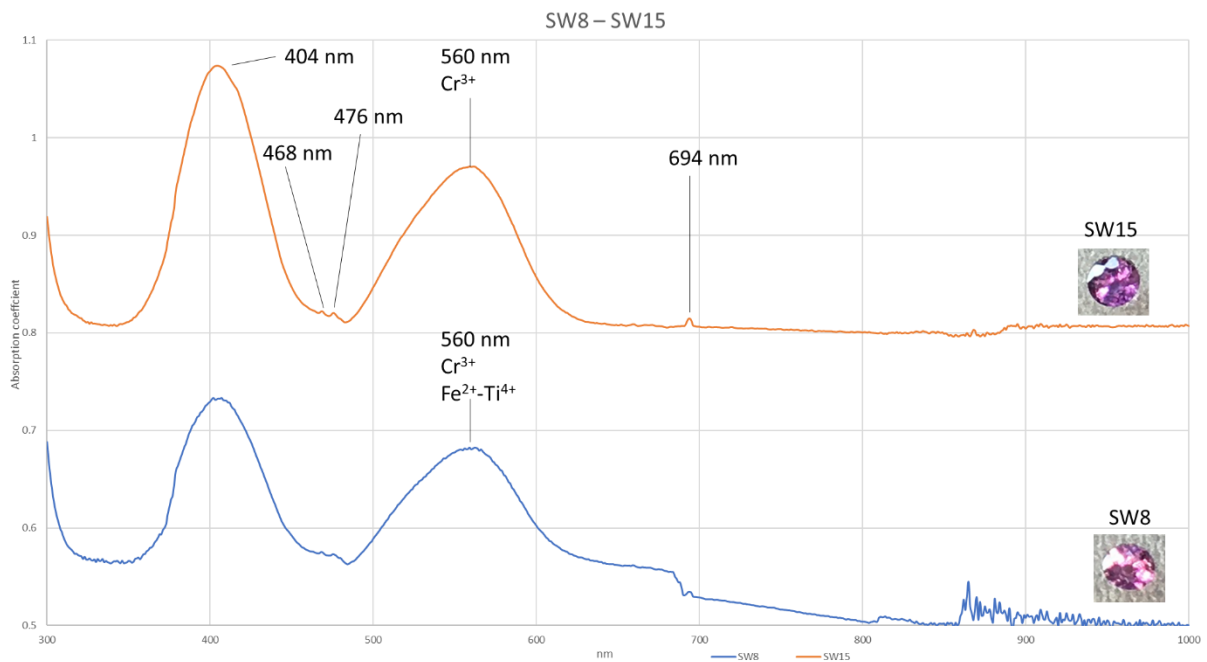


Figure 22: samples SW8 and SW15 have spectra dominated by Cr³⁺. However, in SW8 the Cr³⁺ large band centred at 560 nm is stacked with Fe²⁺-O²⁻-Ti⁴⁺ which is not the case of SW15. No cut off after 300 nm for the two samples. Note in sample SW15 the two small peaks at ~468 and 476 nm due to iron, they are also present in a lot of spectra.

- 4th type (figure 23): the blue sapphires (SW19 and SW20) show spectra dominated by charge transfer Fe²⁺-O²⁻-Ti⁴⁺, and Fe²⁺-O²⁻-Fe³⁺ in one case (SW20).

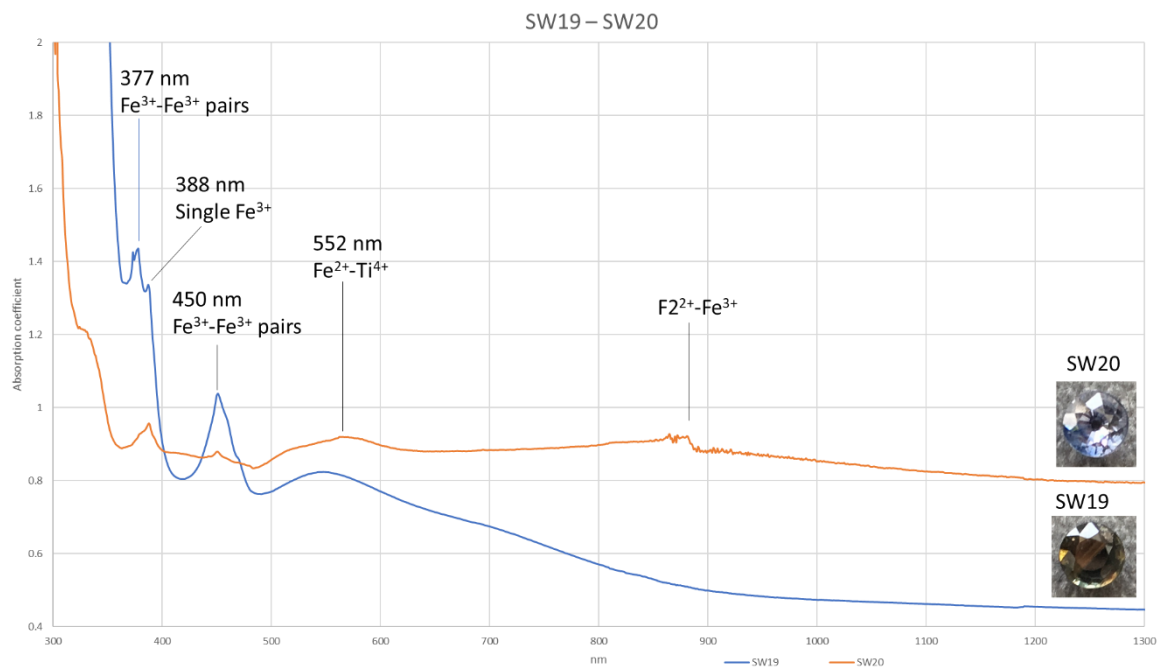


Figure 23: samples SW19 and SW20 show spectra dominated by charge transfer $\text{Fe}^{2+}\text{-O}^{2-}\text{-Ti}^{4+}$ for both of them, and $\text{Fe}^{2+}\text{-O}^{2-}\text{-Fe}^{3+}$ for SW20. Note that SW20 show the shoulder at about 330 nm indicative of a relatively high iron-content

4.2.2 FTIR

The recorded spectra are flat. For a peak to appear, the axis scale was expanded a lot (< 0.1 in absorption coefficient). Therefore, it is not possible to stack several graphs and be able to detect peaks. That is why the spectra are shown individually. Each spectrum presented in the pages below is typical of a series, therefore its interpretation can be extended to other samples.

Despite a truncated culet to get two parallel faces, some spectra are too noisy to be of any use (SW6, SW9, SW10, SW12, SW17). These spectra were redone but they are as noisy as the first one recorded.

Three different types of spectrum can be identified:

- 1st type (figure 24): no particular peak is recorded. Only appear peaks related to isolated carbon dioxide (CO_2) and peaks related to oil, due to sample handling in spite of a thorough cleaning of the stones.

The unrelated CO_2 peaks are around $2,400\text{ cm}^{-1}$ with peaks centred approximately at $2,342$ and $2,362\text{ cm}^{-1}$ (figure 25). They are caused by CO_2 gas present in the environment or in the negative crystals (Phan, 2015).

Oil or fats recorded are generally due to contamination by handling the samples (figure 25). It is characterized by peaks at about $2,853$; $2,924$ and $2,962\text{ cm}^{-1}$ (Cartier, 2009) The spectrum presented below is for sample SW13. The other materials with the same features are SW3, SW4, SW5, SW7, SW8, SW14, SW15 and SW18.

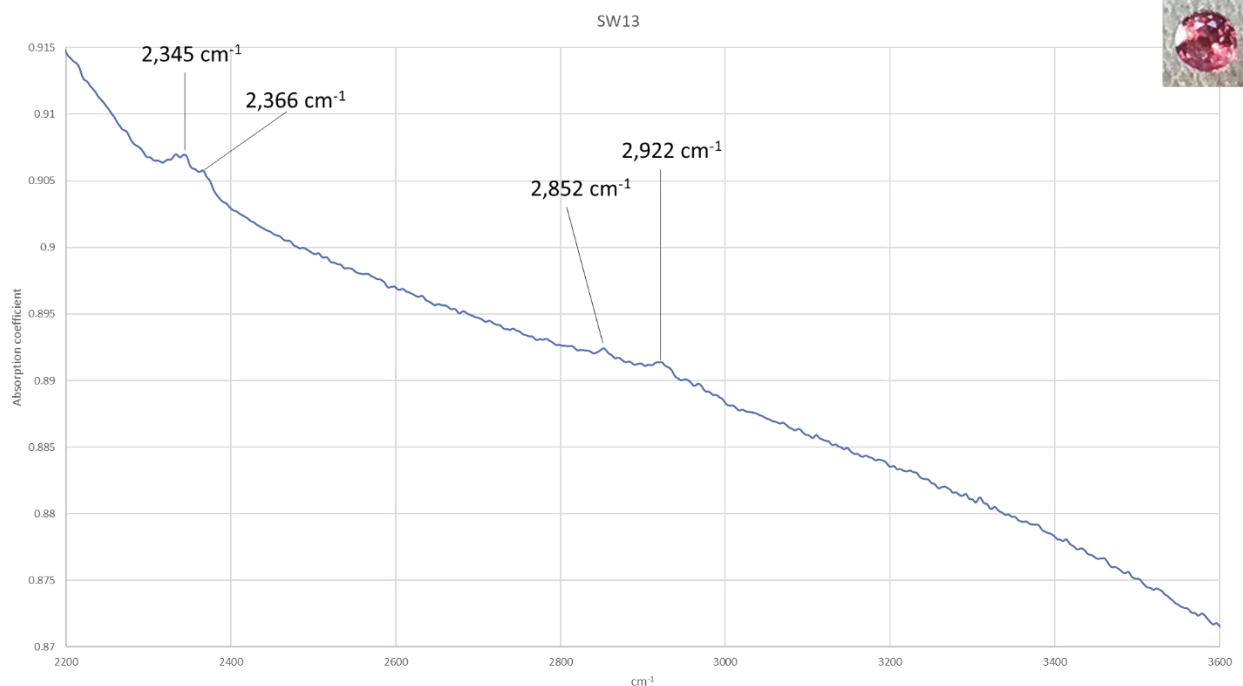


Figure 24: SW13 FTIR spectrum showing nothing more than unrelated CO_2 peaks ($2,345$ and $2,366\text{ cm}^{-1}$) and oil contamination by handling (peaks at $\sim 2,852$ and $2,922\text{ cm}^{-1}$).

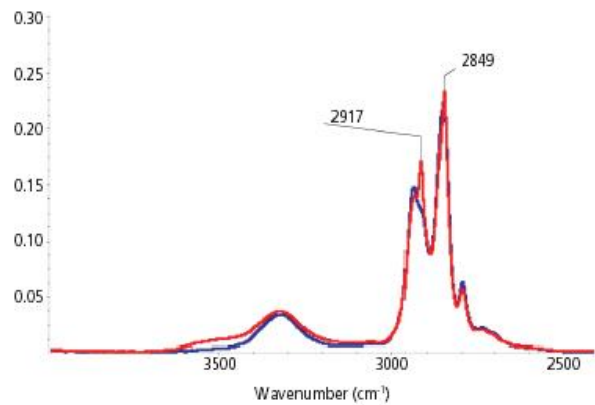
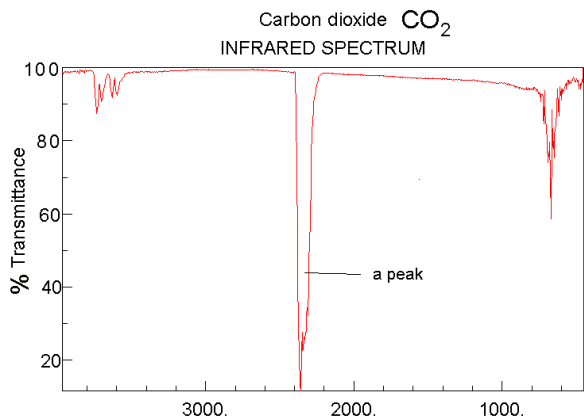


Figure 25: left – CO₂ peak (image taken from <http://webbook.nist.gov/cgi/cbook.cgi?ID=C124389&Type=IR-SPEC&Index=1>), right – peaks related to oil and fats contamination due to handling (image taken from <https://www.azom.com/article.aspx?ArticleID=11722>)

- 2nd type (figure 26): a small peak appears in the OH area, at about 3,309 cm⁻¹. To be able to view this peak, it is necessary to expand a lot the axis scale. The other peaks seen in the 1st type (CO₂, oil and fats) are also present. The spectrum presented below is for sample SW11. The other materials with the same features are SW1, SW2, SW16.

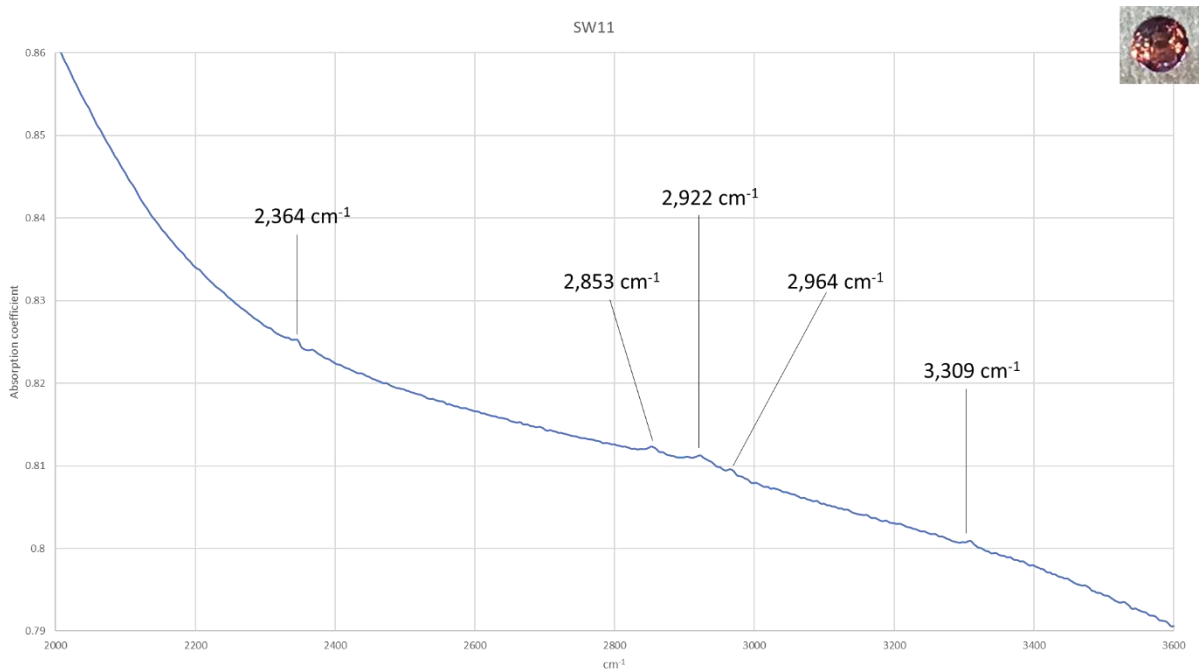


Figure 26: SW11 FTIR spectrum showing a small peak at 3,309 cm⁻¹, unrelated CO₂ peaks and handling contamination peaks are also present

- 3rd type: the blue sapphires (SW19 – figure 27, and SW20 – figure 28) show higher 3,309 cm⁻¹ peaks. Furthermore, they display other peaks related to the 3,309 cm⁻¹. The other peaks seen in the 1st type are also present (CO₂, oil and fats). As there are only two samples, both of them are displayed here.

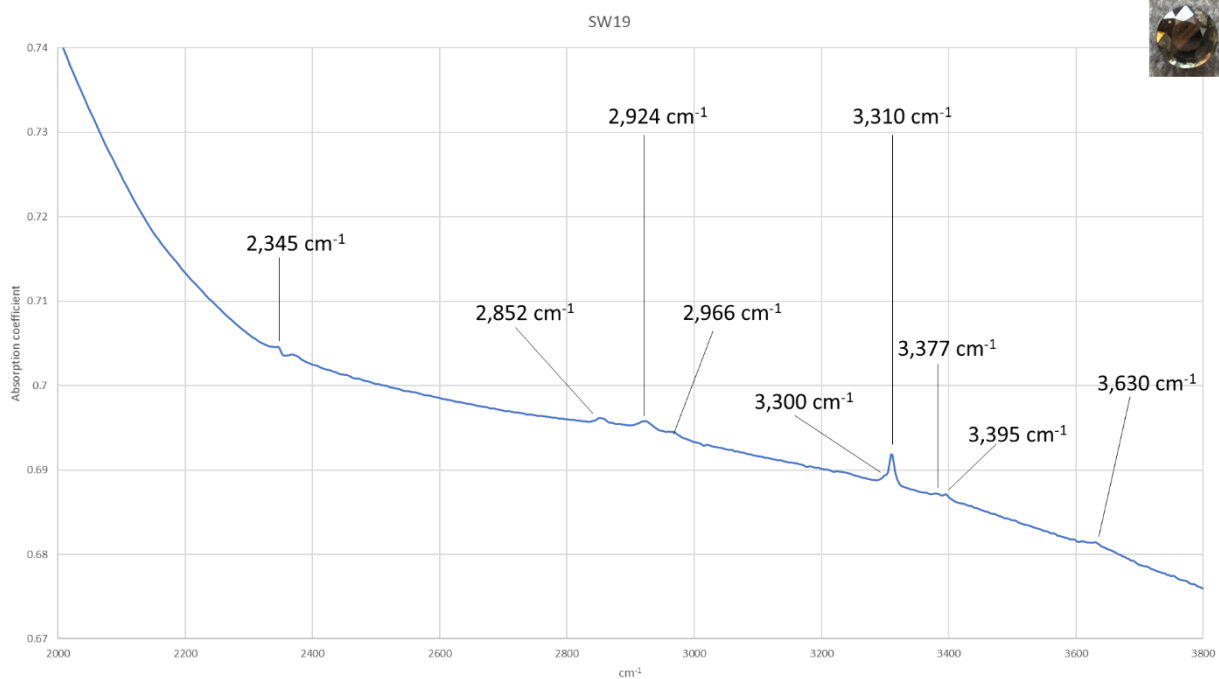


Figure 27: Sample SW19 showing OH-related peaks at 3,300; 3,310 cm⁻¹ and 3,377; 3,395 cm⁻¹. The peak at 3,630 cm⁻¹ has not been identified, but could be related to kaolinite (Scarratt, 2017)

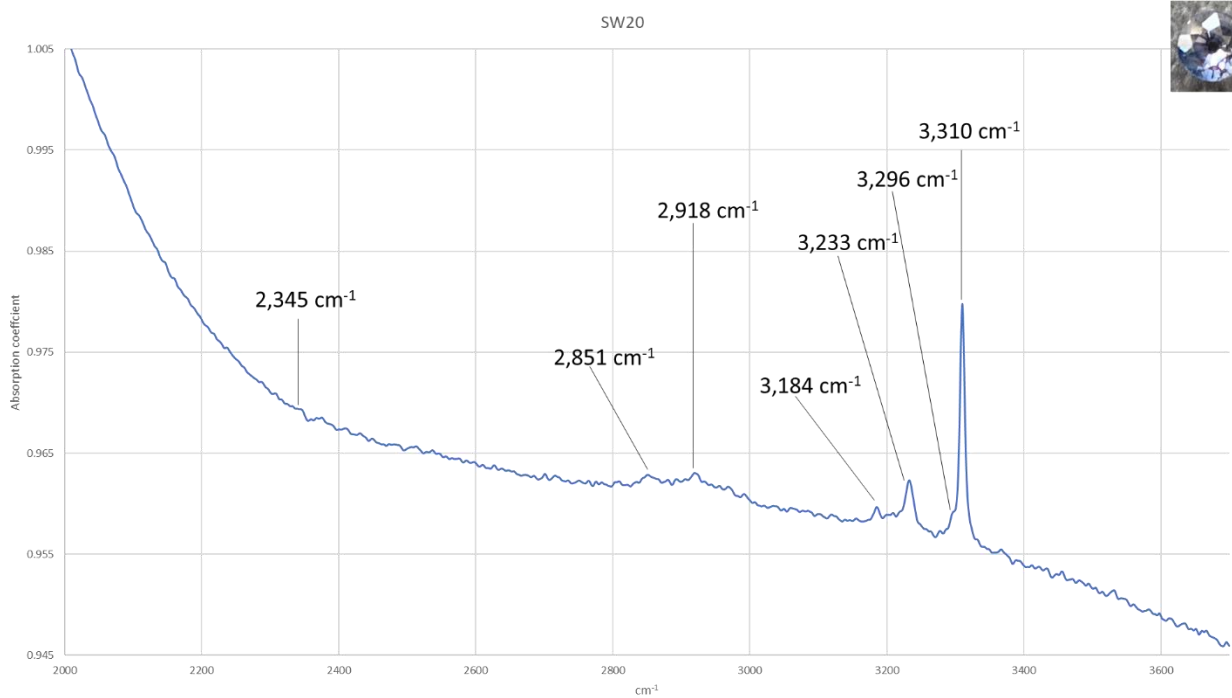


Figure 28: Sample SW20 showing OH related peaks at 3,184 – 3,233 – 3,296 – 3,310 cm⁻¹. The peaks are higher than in any other spectrum

4.3 Chemistry

The results provided by EDXRF are summarized in table 3, below.

Samples	Al ₂ O ₃	CaO	Fe ₂ O ₃	K ₂ O	Cr ₂ O ₃	TiO ₂	Ga ₂ O ₃	V ₂ O ₃	MgO	Na ₂ O
SW1	96.5	1.77	1.06	0.268	0.220	0.165	0.0097	ND	ND	ND
SW2	98.2	1.10	0.200	0.213	0.161	0.0781	0.0268	ND	ND	ND
SW3	96.9	1.52	1.06	0.322	0.115	0.0842	0.0207	ND	ND	ND
SW4	97.0	1.44	0.9520	0.364	0.107	0.120	0.0220	0.0368	ND	ND
SW5	96.8	1.39	1.38	0.315	0.0471	0.109	ND	ND	ND	ND
SW6	96.5	1.90	0.906	0.424	0.169	0.108	0.0151	ND	ND	ND
SW7	97.3	1.25	0.877	0.316	0.074	0.131	0.0152	ND	ND	ND
SW8	97.6	0.926	0.864	0.347	0.227	0.0517	0.0157	ND	ND	ND
SW9	96.1	1.54	1.40	0.271	0.411	0.217	0.0178	0.0277	ND	ND
SW10	95.8	1.83	1.56	0.423	0.265	0.145	ND	ND	ND	ND
SW11	97.2	1.16	1.02	0.329	0.298	ND	ND	ND	ND	ND
SW12	96.7	1.91	0.791	0.311	0.225	0.0734	ND	ND	ND	ND
SW13	96.5	1.68	1.08	0.414	0.177	0.143	ND	ND	ND	ND
SW14	95.1	2.68	1.13	0.634	0.285	0.139	ND	ND	ND	ND
SW15	97.5	1.47	0.17	0.561	0.143	0.110	ND	ND	ND	ND
SW16	97.1	1.34	0.91	0.412	0.117	0.106	ND	ND	ND	ND
SW17	96.9	1.41	0.99	0.615	0.0845	ND	ND	ND	ND	ND
SW18	97.6	1.33	0.66	0.265	0.120	ND	ND	ND	ND	ND
SW19	90.1	6.17	1.93	1.39	ND	ND	0.414	ND	ND	ND
SW20	95.3	2.56	1.06	0.794	0.0276	0.146	0.0622	0.0678	ND	ND

Table 3: data given in mass%. Al₂O₃: aluminum oxide, CaO: calcium oxide, Fe₂O₃: iron oxide, K₂O: potassium oxide, Cr₂O₃: chromium oxide, TiO₂: titanium oxide, Ga₂O₃: gallium oxide, V₂O₃: vanadium oxide, MgO: magnesium oxide, Na₂O: sodium oxide. ND: not detected.

The presence and the high content of calcium is quite surprising, and very unusual. Even if a big calcite inclusion might be present in a sapphire, it would be amazing for it to be present in all of them. Moreover, the EDS function of the SEM never detected any calcium. In these proportions, there is no doubt it would have detected it. This result may come from a contamination during testing and the result for calcium will not be taken into account. With this thought process, potassium may also be ignored.

For some results, such as gallium, it is possible that the equipment did not detect it in some samples. In all the articles published, analyzing corundum with LA – ICP – MS (Laser Ablation – Inductively Coupled Plasma – Mass Spectrometre), gallium was systematically found, of course in small quantity (between 20 and 80 ppm – part per million). So, we can assume that it is present in all corundum in small quantity. The lowest quantity detected is 0.0097 mass% (of gallium oxide), so for computing ratio, I'll just use it below 0.0097 (<0.0097).

A more interactive chemical analysis can be done by using ratio. Several of them have been used, including $\text{Cr}_2\text{O}_3 / \text{Ga}_2\text{O}_3$ vs. $\text{Fe}_2\text{O}_3 / \text{TiO}_2$ (figure 29) or $\text{TiO}_2 / \text{Ga}_2\text{O}_3$ vs. $\text{Fe}_2\text{O}_3 / \text{Cr}_2\text{O}_3$ (figure 30), (Sutherland et al., 1998, Sutherland et al., 2001). These ratios can help separate two different series in magmatic corundum:

- a 'metamorphic' series characterized by a low gallium-content (below 0.015% Ga_2O_3) and a high $\text{Cr}_2\text{O}_3 / \text{Ga}_2\text{O}_3$ ratio (above 4). $\text{Fe}_2\text{O}_3 / \text{Cr}_2\text{O}_3$ should not exceed 10 and $\text{TiO}_2 / \text{Ga}_2\text{O}_3$ should be between 1 and 10. $\text{Fe}_2\text{O}_3 / \text{Cr}_2\text{O}_3$ should range between 1 and 10, as well as $\text{TiO}_2 / \text{Ga}_2\text{O}_3$,
- a 'basaltic' series characterized by a high gallium-content (usually between 0.015 and 0.04% Ga_2O_3) and a low $\text{Cr}_2\text{O}_3 / \text{Ga}_2\text{O}_3$ (always below 1). $\text{Fe}_2\text{O}_3 / \text{Cr}_2\text{O}_3$ should be over 100 (which is not the case for SW20) and $\text{TiO}_2 / \text{Ga}_2\text{O}_3$ should be less than 1.

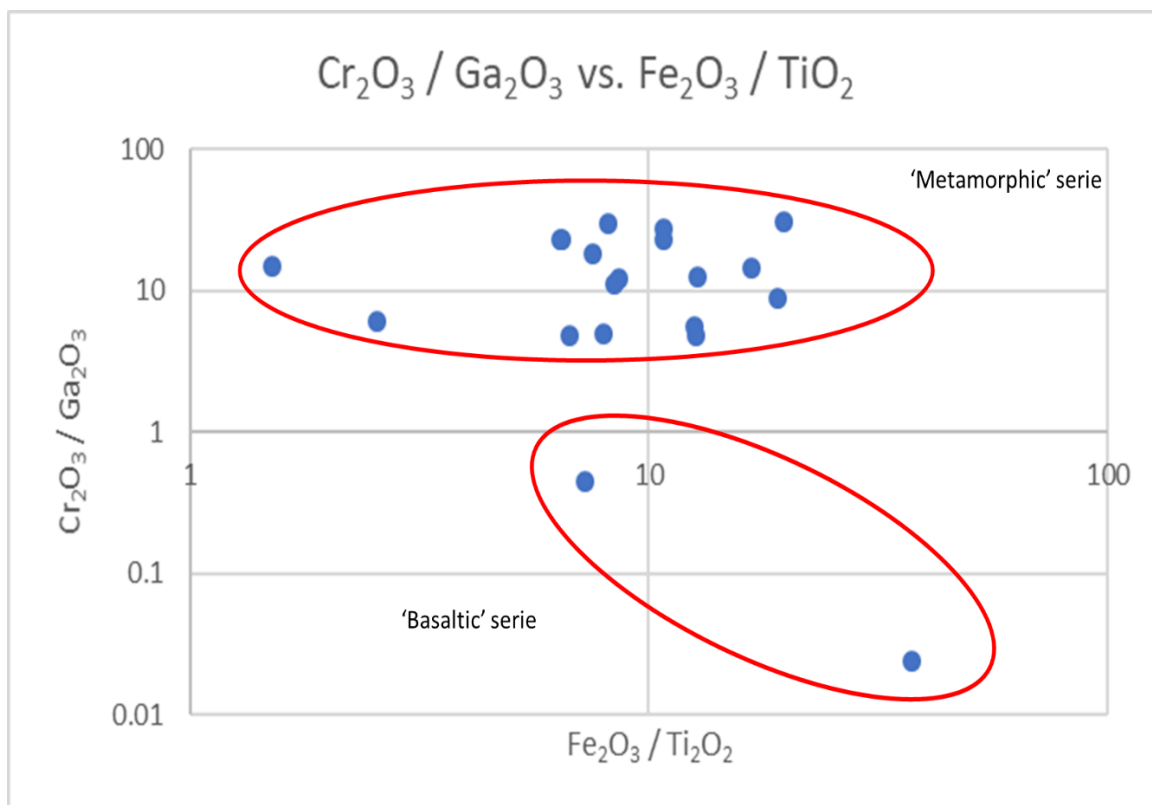


Figure 29: a diagram showing chemical variations plotted to minor and traces elements ($\text{Cr}_2\text{O}_3 / \text{Ga}_2\text{O}_3$ vs. $\text{Fe}_2\text{O}_3 / \text{TiO}_2$). This diagram enables to make a separation between the 'metamorphic' series and the 'basaltic' series. The sapphires belonging to the 'basaltic' series are SW19 and SW20, i.e. the blue sapphires. X and Y axes are on a logarithmic scale (base 10)

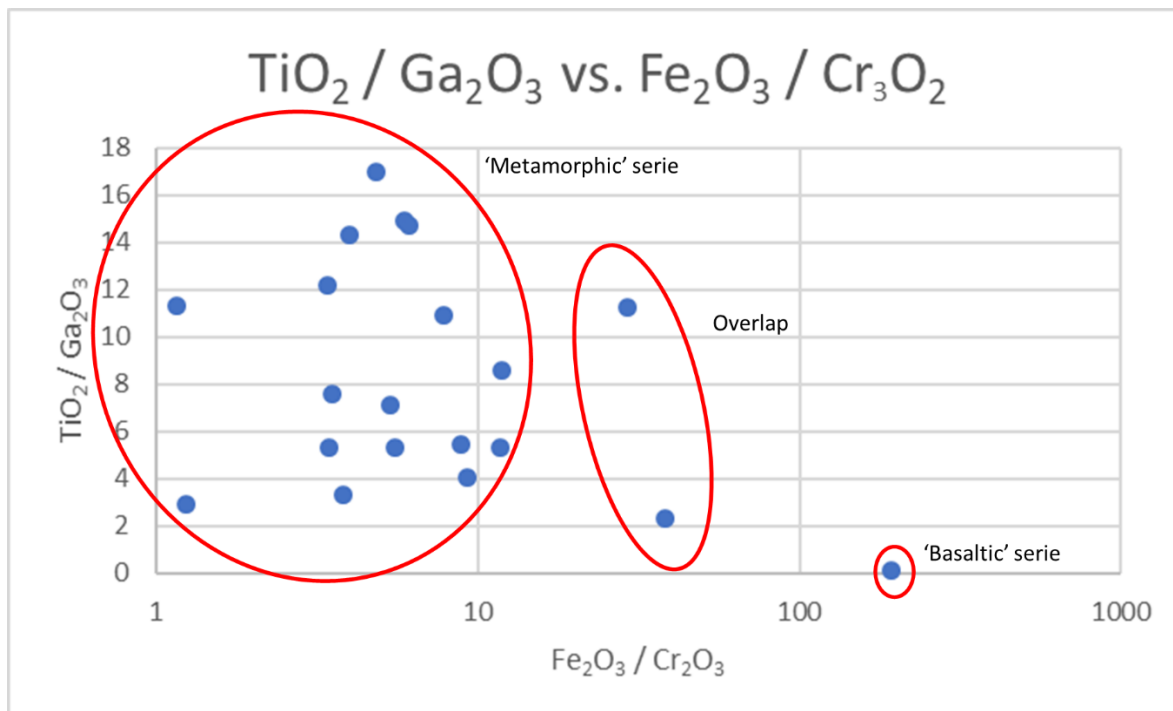


Figure 30: a diagram showing chemical variations plotted to minor and traces elements ($\text{TiO}_2 / \text{Ga}_2\text{O}_3$ vs. $\text{Fe}_2\text{O}_3 / \text{Cr}_2\text{O}_3$). The only one in basaltic series is SW19. With this diagram the separation between the two series is not accurate as $\text{Cr}_2\text{O}_3 / \text{Ga}_2\text{O}_3$ vs. $\text{Fe}_2\text{O}_3 / \text{TiO}_2$. Two overlapping, or in-between (2 out of 20 \rightarrow 10%) results are present: SW5 (top) and SW20 (bottom). X axis only is on a logarithmic scale (base 10)

Other diagrams are frequently used to distinguish between ‘metamorphic’ and ‘basaltic’ series, such as Peucat diagram where chemical variations are plotted against iron and gallium / magnesium (Peucat et al., 2007). Unfortunately, chemical analysis by EDXRF did not detect any trace of magnesium in any of the samples. Therefore, it is not possible to use this valuable tool which might have helped to distinguish more thoroughly between “metamorphic” and “basaltic” series. The use of LA-ICP-MS would certainly enable magnesium to be detected.

5. DISCUSSION

5.1 Colours of the sapphires

In this study, the colours of sapphires can be gathered in three categories:

- purple,
- pink,
- and blue.

The case of sample SW2 which is purple will be treated on its own due to its colour zoning (pink / blue).

As yellow, green and colourless sapphire are barely found in Pailin, the range for fancy colour sapphires is narrower than in any other areas of my knowledge.

5.1.1 PURPLE CATEGORY

Sapphires being purple or having a purplish hue are: SW1, SW2, SW3, SW4, SW5, SW6, SW7, SW8, SW9, SW10 and SW17.

The sapphires from this category are characterized by:

- Cr^{3+} ,
- inter valence charge transfer (IVCT) $\text{Fe}^{2+}\text{-O}^{2-}\text{-Ti}^{4+}$,
- and Fe^{3+} , as single ions or pairs.

Their absorption spectra can be seen in figure 20, and figure 22 for SW8. We have already seen that Cr^{3+} gives a red colour (Fritsch et al., 1987) and $\text{Fe}^{2+}\text{-O}^{2-}\text{-Ti}^{4+}$ gives a blue colour (Fritsch et al., 1988). Therefore, the combination of these two chromophores gives a purple colour.

We also see that the darkest one (SW1 and SW9) have high contents of titanium (table 3) The difference for SW8 is that its spectrum is dominated by chromium, but there is also an absorption of $\text{Fe}^{2+}\text{-O}^{2-}\text{-Ti}^{4+}$. The absorption peak at 377 and 450 nm ($\text{Fe}^{3+}\text{-Fe}^{3+}$ pairs) and 388 nm (single Fe^{3+} ions) are not found. As a result, of this Cr^{3+} predominance, this purple sapphire is the pinkest of its kind.

Furthermore, Fe^{3+} in corundum gives a yellow colour as pairs (Ferguson et al., 1971) or a charge transfer with O^{2-} (Nassau et al., 1987). This yellow colour can be seen as a pleochroic colour carried by the ϵ -ray (table 2). Trapped hole involving Mg associated with Fe^{3+} or Cr^{3+} could also give a yellow pleochroic colour. However, chemical analysis did not detect any result for Mg. And none of the related absorption spectra described by Emmett (Emmett et al., 2017) has been identified in the spectra of figure 20.

5.1.2 PINK CATEGORY

Sapphires being pink are: SW11, SW12, SW13, SW14, SW15, SW16, SW18.

The sapphires from this category are characterized by:

- Cr^{3+} ,
- a lesser intensity, if any, for the inter valence charge transfer (IVCT) $\text{Fe}^{2+}\text{-O}^{2-}\text{-Ti}^{4+}$,
- and Fe^{3+} , as single ions or pairs.

Their absorption spectra can be seen in figure 21, and figure 22 for SW15.

As mentioned already, Cr^{3+} is responsible for the red colour. When the concentration of this chromophore becomes less, the colour has a lighter saturation and turns to the pink (Emmett et al., 2017). As the charge transfer $\text{Fe}^{2+}\text{-O}^{2-}\text{-Ti}^{4+}$ has a lesser intensity, the colour does not move to purple side because the blue component is lesser. Therefore, the gemstone remains mainly pink. Sample SW15 which is strongly dominated by Cr^{3+} is the pinkest (figure 22).

In this pink category, yellow as a pleochroic colour carried by the ϵ -ray has been detected but it tends to be more orange (table 2). For the same reasons as purple "talila", Fe^{3+} is probably the cause of it.

5.1.3 BLUE CATEGORY

Sapphires being blue are: SW19, SW20.

The sapphires from this category are characterized by:

- an inter valence charge transfer (IVCT) $\text{Fe}^{2+}\text{-O}^{2-}\text{-Ti}^{4+}$,
- Fe^{3+} , as single ions or pairs,
- and, an intervalence charge transfer (IVCT) $\text{Fe}^{2+}\text{-O}^{2-}\text{-Fe}^{3+}$ for sample SW20 only.

Their absorption spectra can be seen in figure 23.

The large band of absorption in the near infrared centred at about 880nm is typical of blue basaltic sapphires (Smith, 1978). Alongside with the pair $\text{Fe}^{2+}\text{-Fe}^{3+}$, there is probably a cluster. Indeed, like Fe^{3+} , Fe^{2+} replaces a vacant Al^{3+} site. So, to keep the electrical neutrality of the crystal, a charge must be compensated by an element giving an electron. It could be compensated by Ti^{4+} or Si^{4+} , but there is no good understanding of it (Emmett et al., 2017).

5.1.4 COLOUR ZONING IN SAMPLE SW2

Sample SW2 is purple when viewed face up but shows a pink / blue colour zoning when viewed from the bottom side (figure 14).

Its absorption spectrum (in figure 20-b) shows the same characteristics as purple “talila”, and it also displays a $\text{Fe}^{2+}\text{-O}^{2-}\text{-Fe}^{3+}$ charge transfer.

We can reasonably think that the absorption spectrum is a stack of a pink spectrum (with few or no $\text{Fe}^{2+}\text{-O}^{2-}\text{-Ti}^{4+}$) and blue sapphire (like the one of SW20 – figure 23).

5.2 Geological origin of these sapphires

Magmatic deposits for corundum are mainly secondary deposits. The only primary magmatic deposits are the ones where corundum is associated with syenite (Giuliani et al., 2007).

However, alkali basalt deposit such as Pailin are secondary deposits where corundum is a xenocryst that was carried to the surface when alkali basalt intruded the lenses where corundum formed in crustal extensional zone (Giuliani et al., 2007).

Nevertheless, in alkali basalt deposits, two series from different origin have been identified: a “metamorphic” series and a “basaltic” one.

5.2.1 METAMORPHIC OR BASALTIC?

This series is characterized by a high Cr and low Ga-content (Cr_2O_3 can be up to 0.4-0.5%, and Ga_2O_3 below 0.015%).

The ratios computed on figure 29 identified a “metamorphic” series which is quite distinct from the “basaltic one”. Indeed, based on $\text{Cr}_2\text{O}_3 / \text{Ga}_2\text{O}_3$, if it is above 1 it belongs to the “metamorphic” series, if it is below 1 it belongs to the “basaltic” series (Sutherland et al., 1998). However, for the ratio $\text{TiO}_2 / \text{Ga}_2\text{O}_3$ vs. $\text{Fe}_2\text{O}_3 / \text{Cr}_2\text{O}_3$, the results are less conclusive as they lead to a few overlaps (10% of the sampling). Samples SW5 and SW20 being in between.

Absorption spectra representing a combination of Cr, Fe and Ti peaks and bands are typical of the “metamorphic” series. Therefore, based on this criterion all samples but the blue are from the metamorphic series (see the discussion on colour above). The blue ones ending in the “basaltic” series. If they are “metamorphic” they certainly come from Phnom O Tang area, as it is the only one identified by Sutherland (Sutherland et al., 1998) being active.

5.2.2 QUESTIONS RAISED

Note that SW20 has a little bit of Cr_2O_3 (0.0276%, see table 3) and an emission line can be seen with the hand-held spectroscope, even if it is not the full spectrum (for a chromium spectrum of blue sapphire see specimen-505 page 218 in Hodgkinson, 2015)

Sample SW2 based on $\text{Cr}_2\text{O}_3 / \text{Ga}_2\text{O}_3$ seems to belong to the “metamorphic” series. Even based on $\text{TiO}_2 / \text{Ga}_2\text{O}_3$ vs. $\text{Fe}_2\text{O}_3 / \text{Cr}_2\text{O}_3$, it goes to the “metamorphic” series. And if it is also true that its absorption spectrum combines the Cr, Fe and Ti peaks and bands, the presence of $\text{Fe}^{2+}\text{-O}^{2-}\text{-Fe}^{3+}$ charge transfer introduces some question. Indeed, this large band centred at 880 nm is typical of deep blue basaltic sapphires (Smith, 1978; Emmett et al., 2017). Once again, an accurate diagram such as Peucat ones could help. But this was not possible as Mg was not detected in any sample. But more advanced chemical analysis by LA-ICP-MS would be necessary.

5.3 3,309 cm^{-1} peak and its interpretation

The peak at $3,309 \text{ cm}^{-1}$ is in the OH region. OH group in corundum is structurally bonded to titanium, vanadium, magnesium or iron (Moon et al., 1994). For example, Volynets on a study on synthetic Verneuil corundum showed that the intensity of peaks at $3,160$, $3,233$ and $3,309 \text{ cm}^{-1}$ increases when the amount of silicon, vanadium or titanium increases (Volynets et al., 1972).

Sample SW20 has a mid-infrared spectrum with the highest peak in intensity at $3,309 \text{ cm}^{-1}$. It comes alongside with other peaks $3,184$, $3,233$, $3,296 \text{ cm}^{-1}$. All this peak system is known as the $3,309 \text{ cm}^{-1}$ series (Scarratt, 2017). However, this sample is not heat-treated (figure 17-d).

For the sapphires from the “basaltic” series, the presence of a peak at about $3,309 \text{ cm}^{-1}$ is not a criterion of heat treatment (David et al., 2001). Scarratt gives for illustration the mid-infrared spectrum of an unheated Pailin sapphires with an intense peak at $3,309 \text{ cm}^{-1}$ (figure 31) alongside with its related peak (Scarratt, 2017).

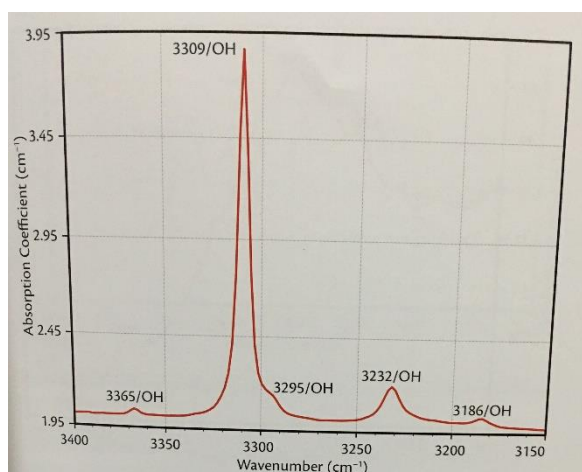


Figure 31: mid-infrared spectrum of an untreated Pailin blue sapphire (figure 4.56 p. 147 in Scarratt, 2017)

“One might normally expect a strong $3,309 \text{ cm}^{-1}$ series to be present in an unheated blue sapphire gained from the basaltic-related deposits in Cambodia (p.147 in Scarratt 2017).

In the sapphires from the “metamorphic” series the signal is very weak or absent (David et al., 2001). In the few spectrum of sapphires, other than the blue ones, where a $3,309 \text{ cm}^{-1}$ peak is present, its intensity is very weak, $0.01\text{-}0.02$ absorption coefficient (figure 26). This observation could reinforce the fact they do belong to the “metamorphic” series.

As mentioned above, the OH are structurally bounded with minor or trace elements. Iron and titanium are hold responsible for the blue colour in corundum. Therefore, the bluer the stone the more visible the $3,309 \text{ cm}^{-1}$ peaks.

For purple stones, the darker ones contain more blue, so they will tend more than other to display a 3,309 cm⁻¹ peak. This is the case for SW1 and SW2, unfortunately spectra of the two other darker stones (SW6 and SW9) are too noisy to be used.

A peak at 3,309 cm⁻¹ cannot be an indication for heat treatment in Pailin materials. In any way, for other gemfields the use of the 3,309 cm⁻¹ peak must be done with care, and be coupled with other test (observation with a microscope for instance).

Eventually, for the “basaltic” series a decrease in intensity of the 3,309 cm⁻¹ peak may be an indication of heat treatment. This has been documented by Pardieu on Mozambique rubies and sapphires. Indeed, a spectrum of the unheated material was recorded. The material was gradually heated and each time an FTIR spectrum was recorded, showing the loss in intensity of the 3,309 cm⁻¹ peak (Pardieu et al., 2015).

CONCLUSION

The goal of this study was to document these fancy colour sapphires known in Cambodia as “talila”.

The analyses made of this material demonstrate the combination effect of chromium, iron and titanium on the colour. The more chromium, the pinker. The more iron and titanium, the purplier.

Some leads on their geological origin have been found, but nothing definitive and more tests, I must confess, with more accuracy, need to be performed to give some certainties to that subject.

Advanced detection of heat treatment using FTIR is not relevant, and one could not shortcut the use of good old microscope on that topic.

While progressing on this study, numerous questions raised remain unanswered: Why yellow, green (the BGY series – blue-green-yellow) and colourless sapphires are barely seen in Pailin when they are quite common actually in Chanthaburi area which is only 60 to 70 miles from Pailin? And due to this difference, is there a way to identify Pailin sapphires from the Thai ones?

ACKNOWLEDGEMENTS

I would like to express my warm thanks to Pr. Emmanuel Fritsch and Dr. Benjamin Rondeau of the University of Nantes for their precious help and advice all along the preparation of this dissertation.

My gratitude goes to Mr. Tay Thye Sun of the Far East Gemological Institute in Singapore for his support and guidance.

I would also like to thoroughly thank Mr. Tan Yee Lang of the national library board in Singapore for helping me get many references.

And of course, all my gratitude goes to my family whose everyday support is invaluable, and particularly to my wife, Evelyne, who was involved and spent so much time trying to decipher my hand-writing and copy the work sheets in a more readable way. She shall also be held responsible for any English grammar or spelling mistakes you may still find in this paper, despite her proof-reading it.

REFERENCES

BOOKS

Emmett J.L., Dubinsky E.V, Hughes R.W., Scarratt K. (2017) Color, spectra & luminescence in Hughes R.W. (2017) Ruby & sapphire, a gemologist's guide, chapter 4, RWH publishing / Lotus publishing, Thailand, pp107-164

Giuliani G., Ohnenstetter D., Garnier V., Fallick A.E., Rakotondrazafy M., Schwarz D. (2007) The geology and genesis of gem corundum deposits in Geology of gem deposits, Groat L.A. edition, Quebec, Canada, Mineralogical association of Canada short course series, vol 37, pp.23-78

Hodgkinson A. (2015) Gem testing technique, Valerie Hodgkinson, Scotland, 542 pages

Hughes R.W. (2017) Ruby & sapphire, a gemologist's guide, chapter 4, RWH publishing / Lotus publishing, Thailand, 738 pages

Scarratt K. (2017) Seeing infrared – Deconstructing the infrared spectra of corundum, in Emmett J.L., Dubinsky E.V, Hughes R.W., Scarratt K. (2017) Color, spectra & luminescence in Hughes R.W. (2017) Ruby & sapphire, a gemologist's guide, chapter 4, RWH publishing / Lotus publishing, Thailand, pp143-149

ARTICLES

Berrangé J.P., Jobbins E.A. (1976) The geology, gemology, mining methods and economic potential of the Pailin ruby and sapphire gem-field, Khmer Republic, Institute of Geological Sciences, Overseas Division, Report No. 35, 32pp. + maps.

Berrangé J.P., Jobbins E.A. (1981) The Pailin ruby and sapphire gemfield, Cambodia, The Journal of Gemmology, vol XVII, 8, pp. 555-567

Cartier L.E. (2009) Ruby and sapphire from Marosely, Madagascar, The Journal of Gemmology, vol 31, n°5-8, pp. 171-179

David C., Fritsch E. (2001) Identification du traitement thermique à haute température des corindons par spectrométrie infra-rouge, Revue de gemmologie, n°141/142, Janvier/Février 2001, pp. 27-31

Fergusson J., Fielding P.E. (1971) The origins of the colours of yellow, green and blue sapphires, Chemical physics letter, vol 10, n°3, pp. 262-265

Fritsch E., Rossman G.R. (1987) An update on color in gems. Part 1: introduction and colors caused by dispersed metal ions, Gems & gemology, Vol. 23, n°3, Fall 1987, pp 126-139

Fritsch E., Rossman G.R. (1988) An update on color in gems. Part 2: colors involving multiple atoms and color centers, Gems & gemology, Vol. 24, n°1, Spring 1988, pp 3-15

Moon A.R., Phillips M.R. (1994) Defect clustering and colour in Fe, Ti: α -Al₂O₃, Journal of the American ceramic society, vol 77, issue 2, February 1994, pp. 356-367

Nassau K., Valente G.K. (1987) The seven types of yellow sapphire and their stability to light, *Gems & Gemology*, vol 23, n°1, pp. 27-35

Pardieu V. (2009) Volume 1: Pailin, Cambodia (Dec 2008 – Feb 2009). GIA laboratory Bangkok, Concise field report, 35 pages

Pardieu V., Saeseaw S., Detroyat S., Raynaud V., Sangsawong S., Bhusrisom T., Engniwat S., Moyal J. (2015) "Low temperature" heat treatment of Mozambique ruby – results report, *GIA research news*, April 28th 2015, 34 pages

Peucat J.J., Ruffault P., Fritsch E., Bouhnik-Le-Coz M., Simonet C., Lasnier B. (2007) Ga/Mg ratio as a new geochemical tool to differentiate magmatic from metamorphic blue sapphires. *Lithos*, vol 98, pp. 261-274

Phan T.M.D. (2015) Internal characteristics, chemical compounds and spectroscopy of sapphire as single crystals. Dissertation, Fachbereich chemie, pharmazie und geowissenschaften der Johannes Gutenberg-Universität Mainz, 148 pages

Smith G. (1978) Evidence for absorption by exchange-coupled Fe²⁺-Fe³⁺ pairs in the near infrared spectra of minerals, *Physics and chemistry of minerals*, vol 3, pp. 375-383

Sutherland F.L., Schwarz D., Jobbins E.A, Coenraads R.R., Webb G. (1998) Distinctive gem corundum suites from discrete basalt fields: a comparative study of Barrington, Australia, and West Pailin, Cambodia, *gemfields*, *The Journal of Gemmology*, vol XXVI, 2, pp 65-85

Sutherland F.L., Schwarz D. (2001) Origin of gem corundums from basaltic fields, *Australian Gemmologist*, vol 21, pp.30-33

Volynets F.K., Sidorova E.A., Stsepuro N.A. (1972) OH-groups in corundum crystals which were grown with the Verneuil technique, *Journal of applied spectroscopy*, vol 17, issue 6, pp. 1626-1628

ANNEX